

A Coalition Game for On-demand Multi-modal 3D Automated Delivery System

Farzan Moosavi^{*a}, Bilal Farooq^a

^a*Laboratory of Innovations in Transportation (LiTrans),
Toronto Metropolitan University, Toronto, Canada*

Abstract

In urban logistics, Unmanned Aerial Vehicles (UAVs) and Autonomous Delivery Robots (ADRs) present promising alternatives for user and eco-friendly delivery solutions, especially when it comes to on-demand delivery. We introduce a multi-modal autonomous delivery optimization framework as a coalition game for a fleet of UAVs and ADRs operating in two overlaying networks to address last-mile delivery in urban environments, including high-density areas, road-based routing, and real-world operational challenges. Establishing the 3D network, a centralized dispatch system is designed to assign optimal delivery modes and determine the routing of the vehicle. The problem is defined as multiple depot pickup and delivery with time windows constrained over operational restrictions, such as vehicle battery limitation, precedence time window, and building obstruction. Subsequently, the coalition game theory is applied to investigate co-operation structures among the modes to capture how strategic collaboration among vehicles can improve overall routing efficiency. To do so, a generalized reinforcement learning model is designed to evaluate the cost-sharing and allocation to different coalitions for which sub-additive property and non-empty core exist. Our methodology leverages an end-to-end deep multi-agent policy gradient method augmented by a novel spatio-temporal adjacency neighbourhood graph attention network and transformer architecture using a heterogeneous edge-enhanced attention model. Conducting several numerical experiments on last-mile delivery applications, the result from the case study in the city of Mississauga shows that despite the incorporation of an extensive network in the graph for two modes and a complex training structure, the model addresses realistic operational constraints and achieves high-quality solutions compared with the existing transformer-based and heuristics methods and can perform well on non-homogeneous data distribution, generalizes well on the different scale and configuration, and demonstrate a robust performance under stochastic scenarios subject to wind speed and direction.

Keywords: On-demand multi-modal pickup and delivery, Coalition game, Deep reinforcement learning, Heterogeneous Graph attention network, Unmanned Aerial Vehicles (UAVs), Autonomous Delivery Robots (ADRs)

1. Introduction

The recent increase in the demand for online shopping and e-commerce has created new challenges toward a resilient logistics supply, specifically in on-demand last-mile delivery in densely populated areas, making it challenging to keep up with the current means of transportation as viable solutions for timely delivery. Thus, reshaping urban logistics cooperatively and effectively can be done to cope with the expected level of service in such situations. In this regard, multi-modal delivery is identified as a promising solution,

*Corresponding author

such as minivans and UAV collaboration (Li et al., 2022), trucks and UAVs (Colajanni et al., 2023), and multi-vehicle truck and ADR delivery (Ostermeier et al., 2023) have been indicated to reduce the utilization of distribution vehicles significantly, timing and operation costs rather than being used individually. Given the complexity of urban environments and dynamically changing conditions, UAV and ADR-based delivery systems are expected to be adopted in the near future (Li and Kunze, 2023). The adoption is further facilitated by the investment in the infrastructure of operational charging facilities, improvements in their technology like batteries and payload capacity, and the development of regulations to ensure safe operations. Moreover, these vehicles reflect superior performance due to their ability to circumvent uncertainties. For instance, Samouh et al. (2020) showed that the hybrid UAV-ADR delivery system offers a higher level of service in various demand and fleet size scenarios, leading to reliable delivery times, which is crucial for on-demand services. Hence, in this study, we leverage the benefit of utilizing UAVs and ADRs as cooperative modes to propose an on-demand multi-modal last-mile delivery framework.

In recent years, the last-mile delivery systems have drastically changed in terms of structure and operations due to the complex nature of the dynamic of urban areas and e-commerce. Besides, various opportunities exist to access certain products daily or hourly, like Amazon Prime service and Uber Eats. This situation stimulates practical solutions for urban multi-modal on-demand routing problems, especially promoting cooperation among these entities in highly populated environments to minimize operational costs and time delay penalties. To do so, we first define a last-mile delivery scope of this research and then implement a game theory model through different coalition groups to investigate the benefit of cooperative modes delivery.

In the context of on-demand delivery, this research considers the multi-depot, multi-vehicle pick-up and delivery problem with time windows (PDPTW) in food delivery. It shows how an NP-hard combinatorial optimization problem with two modes can be solved time-efficiently in the urban environment to account for how on-demand delivery is operated according to the vehicle graph network. We assume that the ADRs operate on the existing sidewalk/bike lane network. Similarly, a predefined virtual network is extended in the air (3rd dimension) for the operations of UAVs designed and managed by the municipality. We aim to minimize the delay in customers receiving their packages by a pickup and drop-off type of delivery through a pre-determined network. Two separate ground and aerial graph networks for ADRs and UAVs are set up, which can travel along the edges. Furthermore, practical assumptions such as weather fluctuation and limited battery and capacity of automated vehicles are considered to capture the realistic aspects of urban delivery.

This research leverages the reinforcement learning (RL) approach for optimization, where agents follow the Markov Decision Property (MDP). A key advantage of learning-based approaches, specifically RL, is their ability to generalize from trained models to solve VRP instances of varying sizes and complexities without redesigning the algorithm or manually adjusting parameters (Bogyrbayeva et al.). Additionally, PDPTW for last-mile delivery is constrained by pairing and precedence relationships, hard pickup, and soft delivery time. Due to its NP-hard nature, it remains difficult for conventional methods, including exact and heuristic algorithms, to solve it optimally in a short computation time (Zong et al., 2022), in which these constraints limit the solution space. On the other hand, deep reinforcement learning (DRL) augmented with a transformer is being used to automatically learn the rules in traditional heuristic methods for solving routing problems, which produces appealing results with much faster computation (Li et al., 2021; Kool et al., 2018). Inspired by them, we aim to solve PDPTW for the various applications of on-demand services, such as food and medicine delivery, by proposing a centralized deep multi-agent reinforcement learning (MARL) approach for coordinating a multi-modal fleet conditioned on the urban environment using dynamic edge-enhanced graph attention network transformer architecture with heterogeneous attention

following the design in Zhang et al. (2023b); Zhang et al. (2022).

Finally, the notion of the core coalition game is brought to this study first to evaluate the cooperating efficiency of two modes if not to operate individually, and second, to promote last-mile delivery companies to form a coalition and collaborate among their vehicles to distribute their operational cost effectively by saving it through fairly allocating the total cost to each coalition. The core coalition theory as a cooperative game theory examines how groups or coalitions form between agents so that no member is incentivized to break from the greater group. The core exists if cost shares in which every coalition member gains a fair share and no smaller group would profit more from acting individually (Chalkiadakis et al., 2022). In this regard, after training the RL model for multi-agent, we use test instances on the generalized model to obtain the core among different coalitions of ADRs and UAVs if the core exists. A coalition game can be formed if the characteristic function satisfies the sub-additivity condition in the grand coalition. A characteristic function evaluates the guaranteed values of all participants' combined costs in a coalition. To ensure such a combination, theoretical properties of the core coalition will be demonstrated for a toy example and then validated through numerical experiments. Note that the core can sometimes be empty, meaning cooperation is not preferred. Thereby, it does not necessarily reduce the total cost or work separately as a more efficient approach.

The rest of this paper is organized as follows: a review of relevant studies and an extensive review of current vehicle routing problems and core coalition game theory are provided in Section 2. Section 3 briefly discusses problem statements, network of operation, and mathematical formulation. Methodology, proposed architecture, coalitional game theory analysis, and core existence are described in Section 4. The application of our proposed framework on the case study and their experimental result are discussed in Section 5. Finally, Section 6 is dedicated to conclusions, final remarks, and future works.

2. Background

2.1. Vehicle Routing Problem

This section reviews the existing literature on traditional heuristic methods and learning-based approaches for routing problems. In addition, the coalition game theory application is reviewed.

Savelsbergh and Sol (1995) was first studied the pickup and delivery problem, and exact methods were proposed as solutions early on Ruland and Rodin (1997), concluding that the dynamic programming performed well on Single-vehicle Pickup and Delivery Problem (PDP) in small-scale instances. On the other hand, attempting to generate exact optimality suffers from heavy computation due to the exponential complexity. As a substitute, more researchers are turning to heuristics to generate approximate optimal solutions, which can significantly increase efficiency while incurring minor quality costs (Zong et al., 2022). For instance, Chu et al. (2021) considered how the food delivery platform can improve by using efficient mini-batching gradient and heuristic algorithms designed to solve the joint order assignment and routing problem of last-mile delivery service in on-demand delivery.

Given the dynamic nature of such an issue, assigning on-demand requests to the best available vehicle on a limited planning horizon is challenging. Liu (2019) comprehensively designed a dynamic rolling horizon for UAV food delivery. Though practical factors such as the orders' location uncertainty, variable demand, carrying capacity, battery consumption, and battery swapping operation have been considered, the computational cost exponentially grows for larger networks.

Even if heuristic-based methods could produce near-optimal solutions in a more reasonable amount of time, they could be more robust in adapting to the new environment; when dealing with high dynamics, the real-time simulation of these methods still needs to be improved. Even though numerous heuristic-based

methods are developed to compute near-optimal solutions, their improvement is not on a larger scale and problem size as they get more time-consuming, and finding efficient rules is still a challenge.

2.1.1. Machine Learning Methods

Lately, there has been a rising inclination to employ deep reinforcement learning for tackling Vehicle Routing Problems (VRPs), and a prevalent characteristic among these approaches is the utilization of a policy network featuring an encoder-decoder structure. Typically, the encoder maps the 2-dimensional locations of customers or nodes into a feature embedding to extract pertinent information from the data. Subsequently, the decoder addresses the problem through either construction or improvement methodologies (Ma et al., 2022). In the construction approach, the decoder initializes with an empty sequence and progressively selects nodes at each step to formulate a complete solution. Conversely, the decoder commences with an already complete initial solution in the improvement approach and continually chooses candidate nodes or heuristic operators for specific operations at each step. This iterative process aims to enhance the solution until the termination criterion is satisfied. A masking scheme is consistently applied to mask the visited or invalid nodes to ensure each customer is visited only once. These Deep Reinforcement Learning (DRL) models can generate higher-quality solutions when augmented with attention mechanisms or graph neural networks.

Reinforcement learning (RL) has found applications in fleet dispatching and management problems such as on-demand delivery and various variants of vehicle routing problems. For example, (Jahanshahi et al., 2022) proposed a meal delivery service as a Markov Decision Process (MDP) and employed Deep Q-Networks (DQN) to optimize courier assignment integrating unique approach of order rejection and repositioning of idle couriers. This work extensively studied the real-time optimization of meal delivery by making order acceptance and courier deployment decisions. Likewise, (Mehra et al., 2023) introduces DeliverAI, a multi-agent reinforcement learning system that allows food delivery networks to provide dynamic routing by providing a novel distributed path-sharing algorithm using Q-learning. However, no graph-based approach was considered, and not all customers will be met by saving on the cost of an order delay in the former. The training process becomes more complex in both cases as models require specialized tuning and can be time-consuming.

Despite their effort to model the complex dynamic of such a problem, PDPTW, as a vehicle routing problem, properly falls into the sequence decision-making optimization, such as encoder and decoder schemes of pointer networks, recurrent neural networks and transformers optimizing by an RL agent. These methods are still modelled as MDP, but they mostly use policy-based methods such as the REINFORCE algorithm or actor-critic architecture to evaluate an action using a combined value-based approach (Williams, 1992). The encoder will process the input data and map them into high-dimensional representation. Subsequently, the decoder outputs each action step by step by extracting information from the internal memory by the design and comparing it with a critical baseline. The first deep learning model for sequential decision-making solution of VRP is introduced by Nazari et al. (2018). Afterwards, this optimization category opened up many research directions to which many scholars have diversely contributed. For instance, Mao et al. (2023) suggested a transformer encoder and LSTM with an attention mechanism for the decoder to model pickup and delivery problems. They used an actor-critic architecture equipped with a Generalized Advantage Estimator that can balance the bias and variance of the policy gradient estimates to show significant improvements over the most competitive baseline on the real-world dataset. Furthermore, James et al. (2019) proposed a novel deep reinforcement learning-based neural pickup and delivery optimization strategy to develop vehicle routing with a pointer network. This work has considered network-based routing, which utilizes the entire graph, not just the customer node, for distance cost calculation. They also study dynamic scenarios where the arrival time of new requests is emulated with a Poisson process and available energy for recharg-

ing changes randomly. Similarly, this study proposed an electric vehicle energy consumption model that considers a variety of factors, such as vehicle power consumption model, road information, and adaptive routing in terms of velocity and node choice based on the time window and physical obstacle, respectively. Regarding the electric vehicle delivery, Liu et al. (2023) proposed a specific UAV delivery problem with recharging characterized by directional edges and stochastic edge costs subject to wind conditions. Fuertes et al. (2023), also utilized multiple UAVs to solve vehicle routing for every agent considering the clustering of the customers and a variant of the Orienteering Problem.

These works either focused on real-world constraints in applying sequential optimization or designed a new algorithm for an RL-enhanced encoder-decoder. Although each gives more importance to one of the urban vehicle delivery aspects, such as routing throughout the entire network, realistic assumption of battery consumption and electric vehicle specification, they ignored incorporating the urban physical structure and dynamic constraints like congestion and obstacle avoidance. As a result, in this research, the scope of the problem is to be solved by RL augmented with a transformer, and the problem framework is defined to encompass a network-based urban vehicle routing problem that considers the dynamic city delivery structure. Furthermore, in the link-level analysis of the network, the edge embedding has been done in Lei et al. (2022) and illustrated that the encoder eventually produces a better node and graph embedding in most instances; thus, the edge-insertion technique in the graph attention will be used as a hop neighbourhood based on spatial and temporal time windows to capture the coupling distribution of the location and demand arrival.

Numerous other works concentrate on the encoder and decoder design while adding complexities like time windows and capacity, for instance, taking into consideration the edge information in the graph structure and residual connections between layers, which is called graph attention networks (GAT) by Veličković et al. (2017). In addition, GAT has shown significant improvements due to its inherent architecture of sharing information through edges; thereby, the entire graph is not required. Besides, Gao et al. (2020) proposed a modified GAT-based network that learns to build better heuristics for VRP and VRP-with-time windows for up to 400 nodes. They utilized a decoder and trained the network with an actor-critic network as an incentive for lower travel costs. Lei et al. (2022) presented edge-encoded GAT with a skip connection (residual E-GAT) at the encoder and used a pointer-based decoder with a self-attention module. Their research shows that edge embedding-based message aggregation has superior graph topology representation power. Likewise, Drori et al. (2020) employed GAT to solve routing problems in linear time. The results showed that the framework can generalize from training on random graphs to running on random and real-world graphs of a different sort. Finally, Zhang et al. (2023b) provided multi-depot vehicle routing problems with soft time windows and encoder-decoder architecture, which employs a graph attention network to extract the complex spatial-temporal correlations within time windows. From these works, it can be concluded that using GAT will reduce the computational burden of the encoding process due to the sparse attention of edges rather than including every single edge in the network. In this regard, Fellek et al. (2023) proposed an attention-based DRL model that learns an expressive graph structure by fusing edge and node information. To that end, the message passing assists in aggregating node features based on data from customer node links. After processing the feature, the encoder produces improved node and graph embeddings. This work reported a close result to the former work of (Lei et al., 2022), which both embedded all the network in the graph. In conclusion, we aim to design a customized heterogeneous GAT as an attention mechanism for pickup and delivery problems, taking the time windows into account to improve the efficiency of the transformer.

2.1.2. Transformer-based Methods

A great deal of research has been done in favour of the transformer detail design to enhance the quality of the result in terms of time, generalization, and scalability. Namely, the work by Rabecq and Chevrier (2022) accounted for capacitated pickup and delivery with time windows problems (CPDPTW) paired with an insertion heuristic that reduces the complexity of the feasibility check from exponential to quadratic. They have used an integrated encoding for the problem features, capacity and time windows. Similarly, Soroka et al. (2023) created CPDPTW and multiple depots and applied a reinforcement learning algorithm based on the Joint Attention Model for Parallel Route-Construction (JAMPR). They take additional routes and vehicle encoders to enrich the context for solving the vehicle routing problem with time windows in the following original work of transformer-based using multi-head attention mechanism (Kool et al., 2018). To do such, JAMPR creates a hidden embedding for each constructed route by embedding nodes and vehicle characteristics of the corresponding route and combining them with the context by the complete representation of the state, allowing multiple routes to be constructed in parallel. Furthermore, Son et al. (2023) proposed a new transformer model, Equity-Transformer, for min-max pickup and delivery routing problems. Such a transformer design contains two key inductive biases: multi-agent positional encoding for order bias and context encoder for equity context. The former considers additional depot nodes mimicking the single agent starting building tours. Conversely, the latter considers crucial factors such as temporal tour length, the target tour length, and the desired number of cities to be visited, thereby enhancing the fairness of the generated tours. Eventually, although work contributed to the vehicle routing field through a novel design and implementation, they did not incorporate the real-world case study or electric vehicle utilization in the urban environment delivery context or cope with multi-agent RL that does not repeat the routing with dummy depot, instead take all agent features into account for matching.

Most existing RL-based techniques, however, can only tackle ordinary VRPs, but the cooperative VRP problem with structural dependency and vehicle cooperation necessitates unique modelling. Li et al. (2021), for example, suggested a heterogeneous attention-based network to tackle single-vehicle PDP; however, cooperative PDP still needs to be solved. In contrast, the suggested Multi-agent PDP could accurately predict pickup-delivery dependencies and vehicle collaborations. On the other hand, these studies by Santiyuda et al. (2024); Zhang et al. (2022); Zhang et al. (2023a) presented the CPDPTW problem by multi-agents which specialize in the assigning and routing of the vehicles simultaneously. Each has designed a unique transformer architecture to account for better input data handling and increased computational efficiency. For example, the encoding approach comprises a joint encoding scheme to encode the spatiotemporal information in the first two, and the latter uses a graph clustering method based on the hop-neighbourhood network. Nevertheless, the decoding step is distinguished by particular context information, making them promising regarding vehicle assignment and checking the compatibility of the vehicle query by each node. Although all of them are composed of paired learning following the (Li et al., 2021) for precedence constraint as well as capacity and time windows, none of them properly addressed more complex constraints and random events in the urban on-demand delivery such as uncertain traffic environments. Furthermore, in the link-level analysis of the network, the edge embedding has been done in Lei et al. (2022) and illustrated that the encoder eventually produces a better node and graph embedding in most instances; thus, the edge-insertion technique in the graph attention will be used as a hop neighbourhood based on spatial and temporal time windows to capture the coupling distribution of the location and demand arrival.

2.2. Vehicle Cooperative Game

In the context of vehicle routing games, core game theory has been applied to various collaborative transportation and delivery problems, particularly focusing on cost-sharing mechanisms. For instance, Osicka et al. (2020) investigated the vehicle routing and location-routing problems (LRP), where decisions

regarding facility location and routing are optimized collectively rather than independently. The study demonstrates that while core allocations are not guaranteed in collaborative location-routing scenarios, they frequently exist in most cases. Cooperative strategies can be beneficial as long as the core is not empty. It also provides insights into how coalition formations impact the viability and stability of shared logistics operations. Note that the cooperative game can be computationally intractable if the number of agents increases as the sub-coalition grows 2^N , where N is the number of agents. Therefore, the cost-sharing allocation for each sub-group can be cumbersome. To this end, Alexander et al. (2014) developed a novel direct coalition induction algorithm (DCIA) method for constructing the characteristic function to ensure that cooperative arrangements first exist and are dynamically stable over time. Additionally, the iterative coalition induction algorithm (ICIA) is introduced to adjust routing plans dynamically, maintaining optimal cooperation throughout the different stages of the game with no coalition having an incentive to leave the grand coalition. Moreover, Zibaei et al. (2016) in the problem of multi-depot vehicle routing problem, incorporated several methods from cooperative game theory, including the Shapely value, the Core, and τ value to allocate the cost savings fairly among the depot owners using numerical examples, where the cost savings and synergy effects of various coalitions are calculated, showing that the cost can be fairly distributed using cooperative game theory techniques. For even more expensive due to the need to solve the NP-hard vehicle routing problem for every possible coalition in the traditional cooperative game theory, Mak et al. (2023) proposed a deep multi-agent reinforcement learning (MARL) model as a coalitional bargaining game. This allows agents to implicitly map coalition formation to collaboration, gain space, and collect fair outcomes without access to the full characteristic function. However, in our research, we aim to find an optimal coalition involving a limited number of agents. Each coalition’s characteristic function comes from a sub-optimal solution to the vehicle routing problem.

The review summary is depicted in Table 1. According to the table, our research has brought several aspects that have yet to be addressed, such as considering the uncertain and stochastic nature of the delivery system and external factors impacting the level of service for a multi-modal fleet in urban real-world constraints. As a result, this study, to the best of the authors’ knowledge, is the first that considers the on-demand food delivery problem modelled by electric-capacitated pickup and delivery with time windows (E-CPDPTW) using dynamic transformer while considering uncertain changes in the urban environment as well as network-based route planning in the presence of wind and physical city structure.

Table 1: Summary of the most relevant studies in the literature

Previous Work	Solution Approach		Problem Characteristic				Model Specification		
	NP	TRL	EV	CVRP	PDPTW	UI	MA	EE	Stochasticity
(James et al., 2019)	✓		✓	✓	✓			✓	✓
(Zhang et al., 2023b)		✓		✓			✓		
(Zhang et al., 2022)		✓		✓	✓		✓		✓
(Elsayed and Mohamed, 2020)	✓		✓			✓	✓		✓
(Zhang et al., 2023a)	✓	✓		✓	✓		✓		
(Lei et al., 2022)		✓	✓	✓				✓	
(Fuertes et al., 2023)	✓	✓	✓	✓			✓		
(Santiyuda et al., 2024)		✓		✓	✓	✓	✓		
Our Study	✓	✓	✓	✓	✓	✓	✓	✓	✓

NP: Network Planning, RL: Transformer Reinforcement Learning, DAM: Dynamic Attention Mechanism, GAT: Graph Attention Network, EV: Electric Vehicle, CVRP: Capacitated Vehicle Routing Problem, PDPTW: Pickup and Delivery with Time Windows, MM: Multi-modal, UI: Urban Infrastructure EE: Edge-embedding, MA: Multi-agent

3. Problem Description

3.1. Setup and Stylized Case Study

In this study, we adopt the transportation network of Mississauga, Canada (Figure 1a) to simulate the pickup and delivery problem with time windows as a food delivery with multiple depots and agents. We obtain data from the OpenStreetMap city map using OSMnx (Boeing, 2017) as the region of interest is shown in Figure 1a, which includes a restricted area due to the presence of the airport near the case study. This network represents the ground on which ADRs and UAVs operate. The street’s intersections denote the nodes connected by corresponding edges. Each edge poses certain transportation features, such as constant path length and real-time traffic speed, resulting in the dynamic travel time associated with each link obtained from the OSMnx Python package. Restaurants as destinations where vehicles would be assigned to pick up food are collected utilizing the web-based data mining tool for Open Street Map, overpass turbine, and the footprint and height of the buildings in the area (Figure 1b). In addition, the demand used in this study is time-dependent based on the time of order during the evening peak and the size of the network after (Samouh et al., 2020).

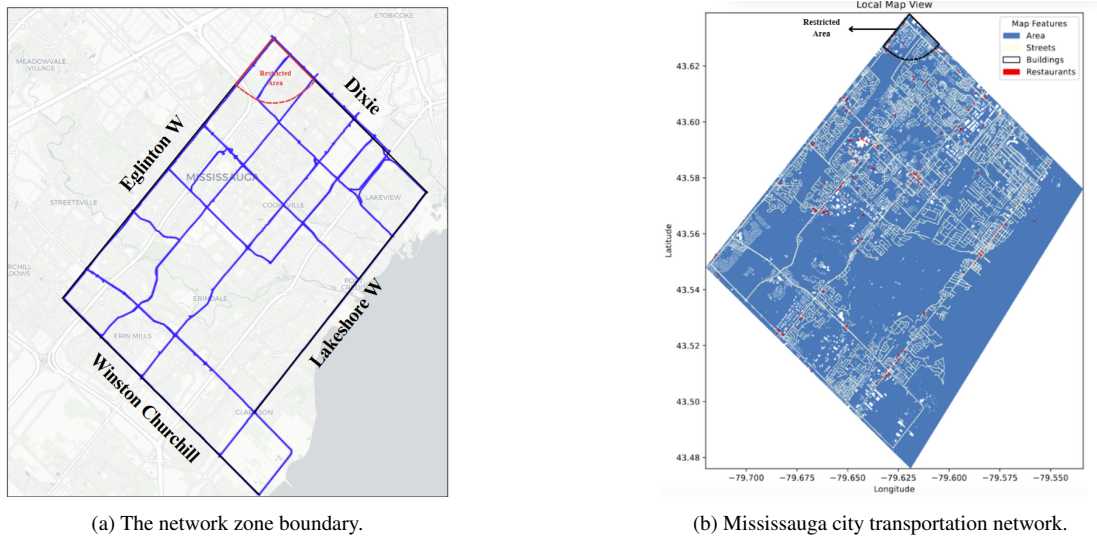


Figure 1: Case study network.

3.2. Cooperative Multi-Modal On-Demand Delivery Problem

Before delving into how the system is optimized to operate sustainably in the urban environment, we must first define how vehicles operate. The ADR traverse along any link except those leading to highways, like primary and secondary roads. This stems from the municipal and safety regulations and operational limitations due to battery constraints. Therefore, the only region allocated to the ADRs is designated residential areas where the ADR can move along sidewalks. The residential edges are in blue in Figure 2, which is part of the case study area better to illustrate the network. On the other hand, the notion of the road network is adopted for aerial delivery. Primary and secondary roads are utilized as the main delivery routes for UAVs, which extend at multiple levels in the airspace with a limit of operation of 400 feet according to the (Osler, 2021). This has the benefit of moving in the structured paths above the roads to bypass the high rises and city infrastructure, as can be visible in Figure 3, which shows a green route for direct delivery or a red path for the next shortest route delivery due to obstruction. The UAV will freely move horizontally

and vertically along the tubes and traverse straight in the absence of obstacles. In this study, optimized performance is considered a move in space during any delivery and take-off and landing occur from a constant level. As a result, the aerial network replicates the double-lane ground roads with the capability of altitude transition at primary intersection nodes. If municipal regulations permit, UAVs can travel through straight lines when the airspace is clear. Otherwise, they move through the edges of the elevated road network as depicted in Figure 3. Similar to ADRs, UAVs pose some limitations in certain areas. For example, the red arced region in Figure 3 shows the restricted circular area near Pearson airport, requiring at least a 5.6 km distance.

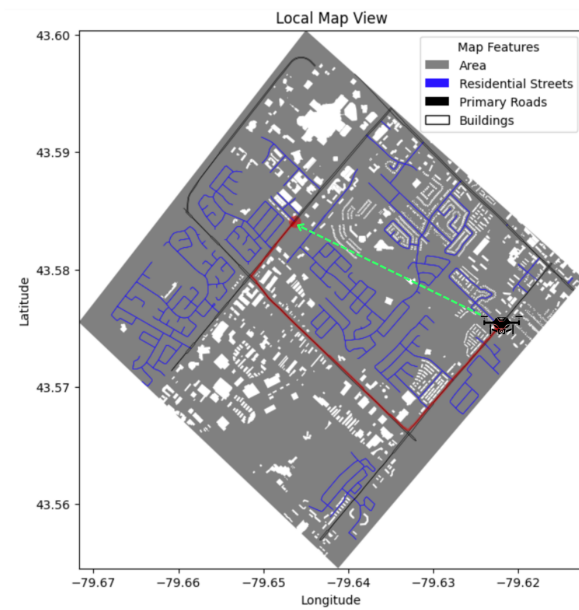


Figure 2: UAV Network Routing

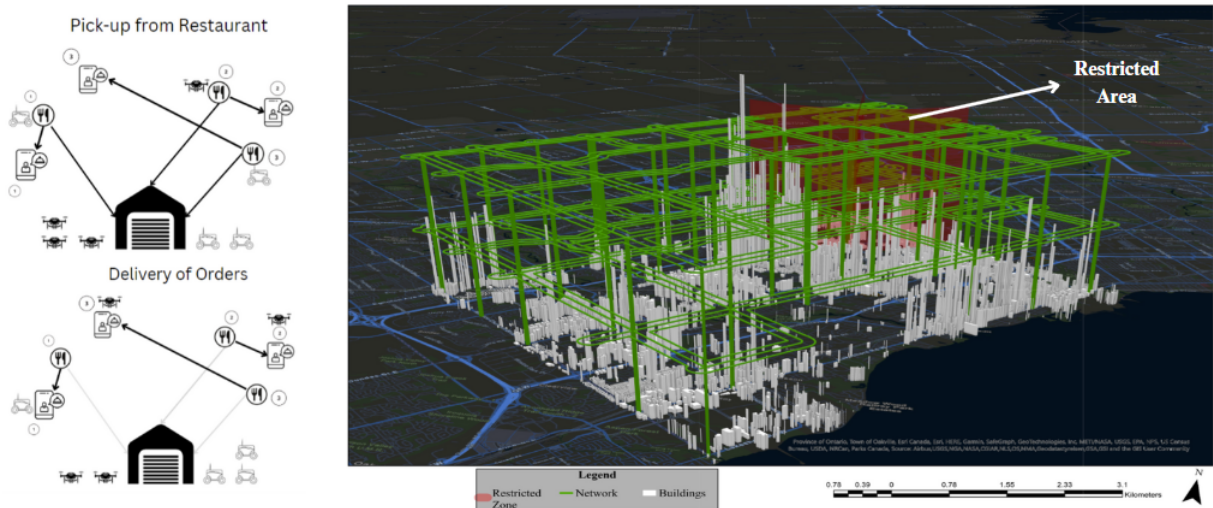


Figure 3: Aerial network for UAVs including restricted zone marked as red arced region

4. Methodology

This section describes how a capacitated pick-up and delivery problem with time windows (CPDPTW) is defined, followed by our solution approach for cost optimization and cooperative strategy. We first present the notation and problem formulation using mathematical expressions as well as a learning-based approach. Next, a vehicle routing game is defined to obtain multi-modal coalition operational costs. The validity of the core properties of coalition theory is confirmed in or obtains an optimal cooperation strategy.

Initially, the delivery problem network comprises two unique graphs for a fleet of UAVs and ADRs based on the road network of an urban area. The nodes are represented by a directed graph for UAV network $G^d = (P \cup D, E^d)$, where $P = \{x_1, \dots, x_N\}$ denotes the set of N pickup nodes, and $D = \{x_{N+1}, \dots, x_{2N}\}$ as corresponding delivery nodes. In addition, $E^d = \{(i, j) \mid x_i, x_j \in X\}$ denotes the set of edges connecting the locations. The same representation is applied for the ADR graph network $G^r = (P \cup D, E^r)$ with the same node but different edges. The coordinate of the i th location, order demand and time window is denoted by \mathbf{u}_i , q_i , and $[e_i, l_i]$ respectively with $q_i > 0$ and $q_{i+N} = -q_i$, for corresponding delivery node. Each vehicle must serve the pickup and delivery of requests together, accounting for precedence constraints within the time window of each point; otherwise, they get delayed, and the penalty is considered. There are N^d and N^r UAVs and ADRs correspondingly. The k th vehicle, $k \in \{1, \dots, N^{d,r}\}$, has a capacity Q_k and a battery size B_k . If the k th vehicle is used, it departs from a depot with a sequence of locations and returns to a depot after its final delivery or when it needs recharging. In other words, a delivery scenario has n customer requests, and each is constituted into a pickup task $i \in P$ and a delivery task $n+N \in D$. A vehicle with a fully charged battery is sent to accomplish all the assigned tasks; the vehicle can be recharged at any depot $c \in C$.

Furthermore, the travel time between any two nodes is the time on the road network based on the impedance weight computed by Dijkstra's algorithm. Note that the vehicle's graph is built upon the customer nodes (pickup and delivery), and every other node is considered an intermediary point that connects these nodes, at which vehicles would not stop. The UAV and ADR networks vary by wind and congestion, respectively, meaning their impedance updates at different times of the day. We adopted the energy consumption model for UAVs in the effect of the wind as proposed in (Liu et al., 2023). Solving the vehicle delivery problem aims to find a route that minimizes the delivery time, including the delay respected to time windows (Santiyuda et al., 2024), while being subjected to constraints regarding the delivery mission and vehicle properties. Further assumptions used in this study are listed as follows:

1. Each customer is served by the same vehicle.
2. Both modes can be assigned for more than one order.
3. Each mode has a certain battery consumption and capacity as well as the battery lower bound threshold to return to the nearest depot for recharging.
4. Each mode can operate within its associated unrestricted network areas.
5. Each vehicle can start from different depots at the first step.

The mathematical notations and formulation of the Electric Pickup and Delivery Problem with Time Windows (E-PDPTW) are proposed as in Appendix A and Table A.5 depicts the variables and parameters definition in this notation. In what follows, the problem model and dynamic are defined by the Markov decision process.

4.1. Markov Decision Process

A generic MDP consists of four components: state space S , action space A , reward function $r(s, a)$, and state transition probability $p(s' \mid s, a)$. Specifically, for the PDPTW described earlier in this paper, these components are defined as follows:

- *States*: Composed of the graph vertex state and the vehicle state, denoted as $s_t = \{x_t, v_t\}$ at step t , where $x_t = (u, q_t, e_t, l_t)$. The k th vehicle state v_t^k is composed of its load u_t , battery level e_t , and traveled time τ^t , expressed as $v_t = [\tau_t^k, u_t^k, e_t^k]$.
- *Actions*: a_t determines the vehicle's node selection at step t . The sequence of actions generated from the initial to the final step should be combinations of nodes starting and ending with the depots.
- *Reward*: PDPTW aims to minimize fleet delay and travel time. Therefore, the reward function is given in Equation 1.

$$R = \alpha_1 \sum_{k \in N^d} \sum_{(i,j) \in N} t_{ijk} X_{ijk} + \alpha_2 \sum_{k \in N^r} \sum_{(i,j) \in N} t_{ijk} X_{ijk} + \sum_{i \in P \cup D} \alpha_3 |T_{ik} - e_i| + \sum_{i \in P \cup D} \max\{T_{ik} - l_i, 0\} \quad (1)$$

Another term, Equation 2, is added to the reward when the agent's energy falls below the battery threshold as a penalty penalizes the agent whose battery has run out. Ensuring efficient behaviour and battery usage encourages the agents to avoid poor routing decisions, leading to increased operational costs and low-battery situations.

$$r_k^t = \lambda R_k^t \quad (2)$$

Where λ is a positive coefficient, and R_k^t is the reward of the agent k at step t .

- *Transition*: The system state will be updated from S_t to S_{t+1} based on the currently executed action a_t . The dynamic features of the problem, such as vehicle load, battery level, and travelled time, are being changed through consecutive nodes based on the vehicle's features (Equations 3, 4, 5, and 6). First, the system time is updated based on these equations.

$$\tau^{t+1} = \begin{cases} \max(\tau^t, l_i) + s + t_{ijk}, & \text{if } i \in P \cup D \\ \tau^t + (B^k - e_i^k) / \eta_k + t_{ijk}, & \text{if } i \in C \end{cases} \quad (3)$$

where η_k is the charging rate to charge the battery from the given level for any vehicle k , s is a constant representing the service time at each customer vertex. Next, the battery level of the vehicle is updated:

$$e^{t+1} = \begin{cases} e^t - e_{ijk}, & \text{if } i \in P \cup D \\ B^k, & \text{if } i \in C \end{cases} \quad (4)$$

Where e_{ijk} is the energy consumption of the vehicle k travelling from vertex i to vertex j . The power consumption model for UAV and ADR batteries is discussed in Appendix B.

Finally, the vehicles load u^t , and the remaining demand, d_i^t , at each vertex are updated as follows.

$$u^{t+1} = \begin{cases} u^t + d_i^t, & \text{if } (i \in P) \cap (\tau^t \in [e_i, l_i]) \\ u^t - d_i^t, & \text{if } (i \in D) \cap (\tau^t \in [e_i, l_i]) \\ u^t, & \text{if } i \in C \end{cases} \quad (5)$$

$$d_i^{t+1} = \begin{cases} 0, & \text{if } (i \in P \cup D) \cap (\tau^t \in [e_i, l_i]) \\ d_i^t, & \text{if } i \in C \end{cases} \quad (6)$$

- *Policy*: The stochastic policy p_θ automatically selects a node at each time step under the precedence constraint. This process is repeated iteratively until all pickup-delivery services are completed. The final outcome engendered by performing the policy is a permutation of all nodes, which prescribes the order of each node for the vehicle to visit, i.e., $\pi = \{\pi_0, \pi_1, \dots, \pi_T\}$. Based on the chain rule, the probability of an output solution is factorized as Equation 7.

$$P(\pi | X) = \prod_{t=0}^{T-1} p_\theta(\pi_t | X, \pi_{1:t-1}) \quad (7)$$

where X is the input of a problem instance. The decision-making about the node selection will be performed based on the learned p_θ .

Afterwards, the detailed architecture of the transformer and elements of the encoder and decoder are elaborated.

4.2. Reinforcement Learning Approach

This study integrates a Graph Attention Network (GAT) and Transformer architecture to address these challenges using an end-to-end learning approach. Deep reinforcement learning (DRL), augmented with a dynamic transformer model and a novel customized graph attention network, solves PDPTW and minimizes the delivery time delay. The proposed approach coordinates a multi-modal fleet with a network on the ground and in the air, using a dual encoder architecture to capture the embedding of both modes, along with heterogeneous attention to account for precedence constraints (Zhang et al., 2022) and, more importantly, a customer's spatial and temporal correlation to enrich node and graph context embedding for dynamic routing. A dynamic encoding mechanism is introduced to update edges in addition to node embedding, serving as a dynamic encoder that reflects the online routing problem and addresses on-demand delivery. The flowchart of this methodology is shown in the Figure 4.

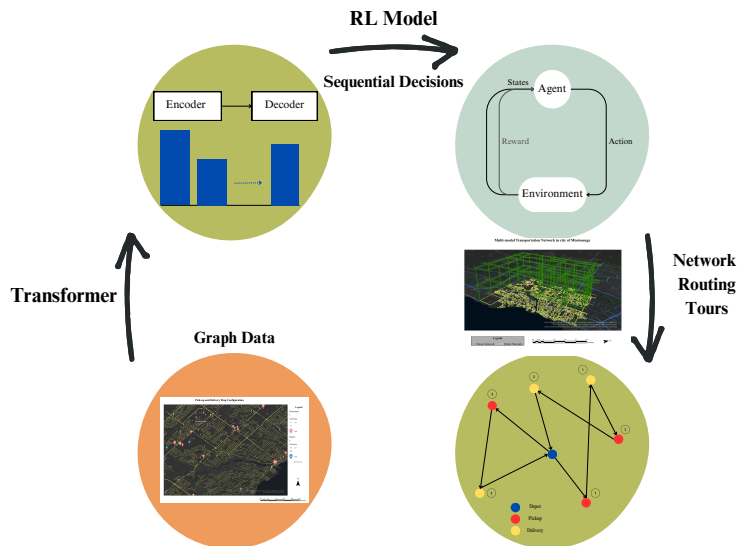


Figure 4: The process of routing problem solution

4.2.1. Graph Attention Encoder

According to Figure 5, the method comprises graph attention encoding part moving to the cooperative decoding for handling both fleets. Before the encoder, the time and distance-based hop neighbourhood for edges are incorporated to find a spatial-temporal correlation for aerial and terrestrial network embedding.

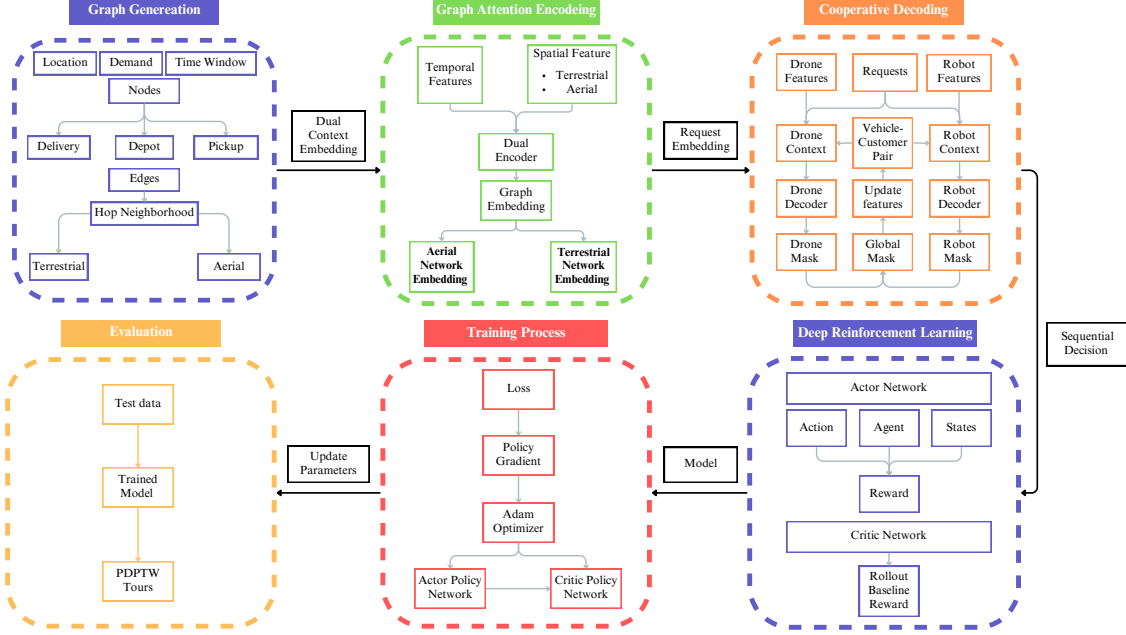


Figure 5: Overview of the methodology

The incorporation of attention layers builds upon the recent work Zhang et al. (2023b); Kool et al. (2018). An adjacency matrices of temporal distribution are defined as $A_{i,j} = 1$ if the time window of the two customers is close and if the late time window l_i of customer x_i is nearest to late time window l_j of customer x_j ; otherwise, $A_{i,j} = 0$. The temporal and spatial adjacency neighbourhood for a node x_i is defined by NB_i^T and NB_i^S , which limits the neighbourhood in adjacency matrices with a time window by a threshold ζ and distance threshold by μ , for UAVs and ADRs respectively. In addition, a parameter called density, ρ , is defined to determine the probability of how dense the environment is, namely, the existence of an obstacle along two connecting nodes. A broad spectrum of customers' time and space correlation can be trained by tuning these thresholds and testing various scenarios, such as sparse and dense urban environments. First, the initial embedding for each node and fleet edges is computed in Equation 8 and 9 through a linear layer.

$$\mathbf{h}_i^0 = \begin{cases} \text{BN}(\mathbf{W}_1(\mathbf{x}_i; \mathbf{x}_{i+N}) + \mathbf{b}_1), & \text{if } i \in \{1, \dots, N\}, \\ \text{BN}(\mathbf{W}_2(\mathbf{x}_i) + \mathbf{b}_2), & \text{if } i \in \{0, N+1, \dots, 2N\} \end{cases} \quad (8)$$

$$\mathbf{e}_{ij}^d = \text{BN}(\mathbf{W}_3 E_{ij}^d + \mathbf{b}_3), \mathbf{e}_{ij}^r = \text{BN}(\mathbf{W}_4 E_{ij}^r + \mathbf{b}_4), \text{ if } i, j \in NB_i^T \quad (9)$$

where $\mathbf{W}_1, \mathbf{W}_2, \mathbf{W}_3, \mathbf{W}_4, \mathbf{b}_1, \mathbf{b}_2, \mathbf{b}_3,$ and \mathbf{b}_4 represents the learnable parameters and $\text{BN}(\cdot)$ represent batch normalization. The graph attention network can assign different importance to the customers within the neighbourhood based on the node role through the attention mechanism (Lei et al., 2022) by computing the pairwise attention weight a^{ij} at l th layer as in Equations 10 and 11. In this setup, we have defined the

attention weight in a time dimension manner, capturing the vehicle's travelling ability as well. In other words, each connecting edge weight in the graph attention network is considered as the relative time that can be passed by a certain vehicle within the time window between two nodes. Therefore, $\hat{e}_{ij}^d = \left| e_i - l_j - \frac{d_{ij}}{v_d} \right|$ for UAVs and $\hat{e}_{ij}^r = \left| e_i - l_j - \frac{d_{ij}}{v_r} \right|$ exist for ADRs. Where d_{ij} is the shortest distance between node i and j , v_d and v_r are the UAV and ADR maximum velocities, respectively. This configuration has been a trade-off between the case of time-window and distance proximity, leading to better convergence for training dual complex encoding schemes by incorporating the network and vehicle specifications so each node can gain a meaningful, distinguished, and absorbing heterogeneous embedding.

By doing so, each pickup node would be influenced by the corresponding delivery and potential close-time proximity of other pickup nodes.

$$\alpha_{ij|P}^\ell = \frac{\exp\left(\sigma\left(\mathbf{g}_1^{\ell T} \left[\mathbf{W}_1^\ell \left(\mathbf{h}_i^{(\ell-1)} \parallel \mathbf{h}_j^{(\ell-1)} \parallel \hat{e}_{ij} \right) \right]\right)\right)}{\sum_{z \in NB_i^T \cup NB_i^S} \exp\left(\sigma\left(\mathbf{g}_1^{\ell T} \left[\mathbf{W}_1^\ell \left(\mathbf{h}_i^{(\ell-1)} \parallel \mathbf{h}_z^{(\ell-1)} \parallel \hat{e}_{iz} \right) \right]\right)\right)} \text{ if } (i \in P, j \in P \cup D) \quad (10)$$

$$\alpha_{ij|D}^\ell = \frac{\exp\left(\sigma\left(\mathbf{g}_2^{\ell T} \left[\mathbf{W}_2^\ell \left(\mathbf{h}_i^{(\ell-1)} \parallel \mathbf{h}_j^{(\ell-1)} \parallel \hat{e}_{ij} \right) \right]\right)\right)}{\sum_{z \in NB_i^T \cup NB_i^S} \exp\left(\sigma\left(\mathbf{g}_2^{\ell T} \left[\mathbf{W}_2^\ell \left(\mathbf{h}_i^{(\ell-1)} \parallel \mathbf{h}_z^{(\ell-1)} \parallel \hat{e}_{iz} \right) \right]\right)\right)} \text{ if } (i \in D, j \in P \cup D) \quad (11)$$

where $(\cdot)^T$ represents transposition, \parallel is the concatenation operation, $\mathbf{g}_1^\ell, \mathbf{g}_2^\ell$ and $\mathbf{W}_1^\ell, \mathbf{W}_2^\ell$ are learnable weight vectors and matrices respectively, and $\sigma(\cdot)$ is the softmax activation function. Subsequently, the final embedding for each node will consist of parts including pickup and delivery paired attention and all the nodes' attention with a non-shareable weight parameter of \mathbf{W}_l^V , in Equation 15. Afterwards, we use feed-forward with a residual connection and BN layer followed by calculating K multi-head attention of the weight value vector for l th layer in Equations 12, 13, and 14

$$\widehat{\mathbf{h}}_i^{(1)} = \text{BN} \left(\mathbf{h}_i^{(0)} + \sum_{k=1}^K \mathbf{W}_3^k \mathbf{h}_i' \right) \quad (12)$$

$$\mathbf{h}_i^{(1)} = \text{BN} \left(\widehat{\mathbf{h}}_i^{(1)} + \varphi \left(\widehat{\mathbf{h}}_i^{(1)} \right) \right) \quad (13)$$

$$\varphi(\mathbf{x}) = \text{ReLU}(\mathbf{W}_5 \mathbf{x} + \mathbf{b}_2) \quad (14)$$

$$\mathbf{h}_i^l = \sum_{j \in NB_i^T \cup NB_i^S \cup D} a_{ij|P \cup D} \mathbf{W}_l^V \mathbf{h}_j^{(l-1)} + \sum_{j \in NB_i^T \cup NB_i^S \cup P} a_{ij|P} \mathbf{W}_l^V \mathbf{h}_j^{(l-1)} + \sum_{j \in NB_i^T \cup NB_i^S \cup D} a_{ij|D} \mathbf{W}_l^V \mathbf{h}_j^{(l-1)} \quad (15)$$

As the output of the attention mechanism to get the final and average embedding shown in Equation 16, note that ADRs and UAVs do not share parameters through the encoding mechanism and are embedded separately with unique network configurations. Figure 6 illustrates a detailed design of the encoder.

$$\mathbf{h}_j = \frac{1}{n} \sum_{i \in P \cup D} (\mathbf{h}_i^l)_j \quad (16)$$

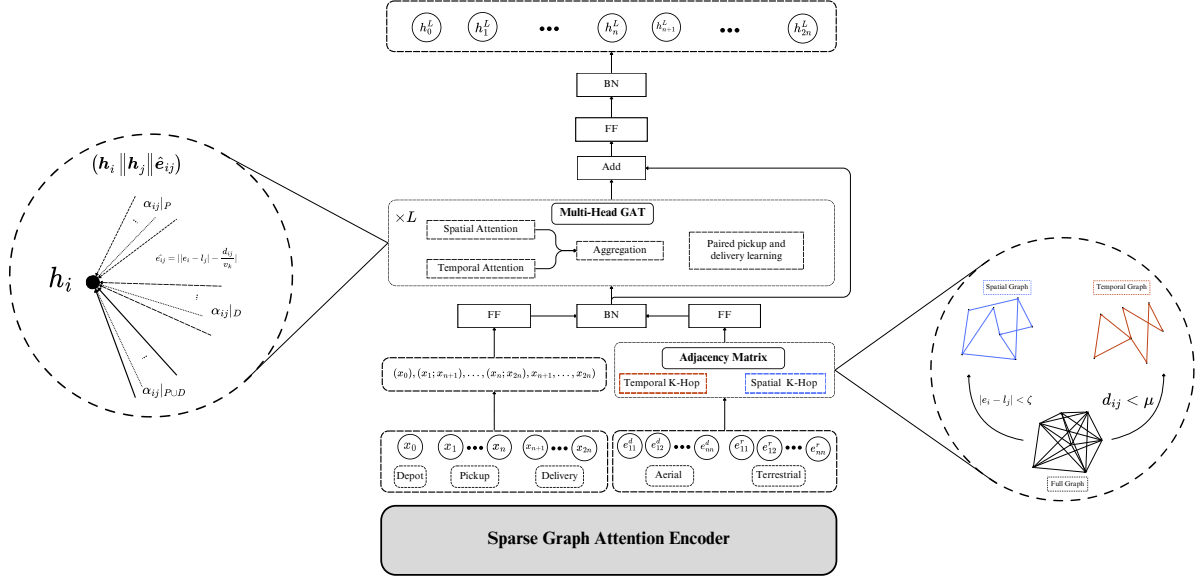


Figure 6: The encoder architecture and graph attention adjacency mechanism

4.2.2. Decoder

In the decoder, the context embedding of each vehicle will be aggregated by fleet states concatenated with node embedding to get agent embedding as Equation 17.

$$\mathbf{x}_k^{(a)} = \mathbf{v}_{k,t} + \mathbf{W}_5 \cdot [\bar{\mathbf{h}}(N); \mathbf{v}_{1,t}; \mathbf{v}_{2,t}; \dots; \mathbf{v}_{K,t}], \quad \forall k \in N^d, N^r. \quad (17)$$

We define the query vector as the agent embedding $\mathbf{x}_k^{(a)}$, key vectors and value vectors as the customer embedding \mathbf{h}_i , and utilize the attention mechanism to compute the importance $u_{k,i}$ of each customer i to agent k as in Equation 18.

$$u_{k,i} = (\mathbf{W}_6 \cdot \mathbf{x}_k^{(a)})^T \cdot (\mathbf{W}_7 \cdot \mathbf{h}_i), \quad \forall i \in N, \quad \forall k \in N^d, N^r \quad (18)$$

Next, we calculate the agent-customer joint information embedding as the weighted sum of value vectors in Equation 19.

$$\mathbf{h}_{v,k} = \sum_{j \in N} \frac{e^{u_{k,j}}}{\sum_{j \in N} e^{u_{k,j}}} \cdot \mathbf{V}_j, \quad \forall k \in N^d, N^r. \quad (19)$$

Furthermore, the decoding process encodes the joint information embedding to a query (Zhang et al., 2022). To do so, compare it with each customer's key to acquire the attention coefficient, representing the compatibility between vehicle k and customer i at time t , according to Equation 20.

$$\tilde{h}_{k,i} = (\mathbf{W}_8 \cdot \mathbf{h}_{v,k})^T \cdot (\mathbf{W}_9 \cdot \mathbf{h}_i), \quad \forall i \in N, \quad \forall k \in N^d, N^r. \quad (20)$$

To guarantee that each vehicle would not select the same node, a global mask is used to handle such situations and other operational and delivery constraints; the masking procedure is used for both fleets in the probability of the selecting node i , which is noted in Equation 21:

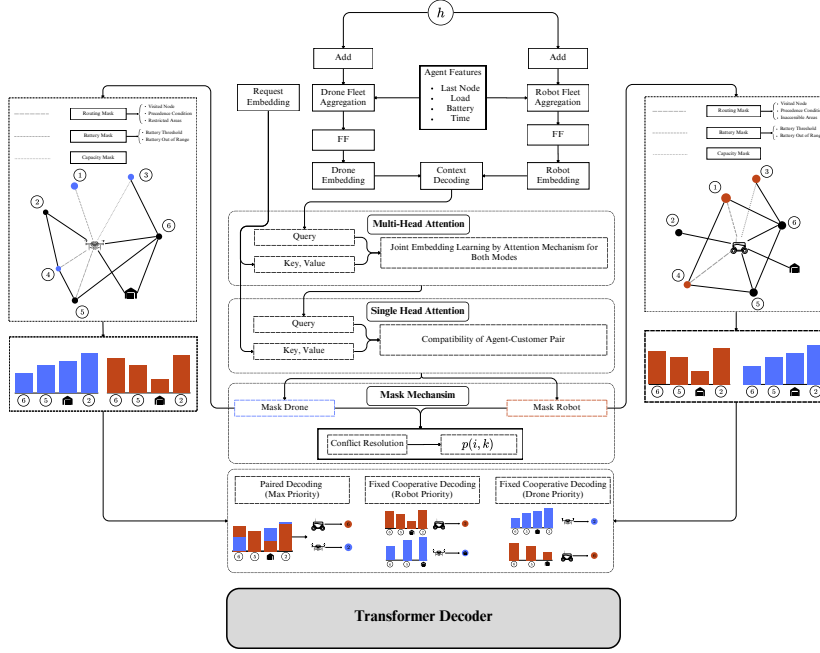


Figure 7: The decoder architecture strategies and masking scheme representation

$$P(i, k) = \text{softmax}(C \cdot \tanh(\tilde{h}_{k,i})) \quad (21)$$

with Clip parameter of C , and W_5, W_6, W_7, W_8, W_9 are learnable weight parameters. As a result, a tour can be generated by selecting vehicle-node pairs at every step. The output will be given to the encoder for re-encode the states to account for removing the visited node and re-embedding the edges states to update to features of the network; thereby, the decoder can be influenced by a variation on network embedding at the decoding step to select the superior pair. The detailed design of the decoder is depicted in Figure 7. In the assignment step, three strategies were adopted to test if a priority-based model in the decoding stage would perform superiorly in contrast to joint learning. The latter is when a node is assigned to the highest probability in two modes, whereas the former is for either of the modes; there is a priority in the assignment, and the UAV-priority case is at less risk due to versatility over ADRs in normal delivery situations.

4.2.3. Masking Scheme

To ensure every node assignment to an available vehicle is feasible, a set of masking rules will be applied before the final step of the decoder. This way, only unmasked nodes and vehicles will remain in the probability of Equation 21. The mask rules consist of the following.

- Each node is visited only once, except for charging stations.
- Each vehicle must be reachable to a customer within its remaining load and battery capacity.
- The vehicle capacity must accommodate the request for the whole trip; it would return to depots if it cannot service any two sets of pickup and delivery nodes.

- The out-of-range nodes will be masked based on the temporal and spatial adjacency neighbourhood threshold.
- For any pickup node, all delivery nodes, except the corresponding one, will be masked.

Figure 8 illustrates a visualization case of masking steps. Red and blue area networks account for the ADRs and UAVs, respectively, which in the first step can let each mode access more customers. In contrast, in the third step, the coverage radius is lowered due to operational constraints like battery shortages. Both mode network coverage is limiting due to node restriction of how the masking algorithm applies to accessible nodes. There are, in this case, three depots throughout the map where either of the mode can begin operating, by taking each step of the routing, the network coverage that a delivery service is available is gone under variation.

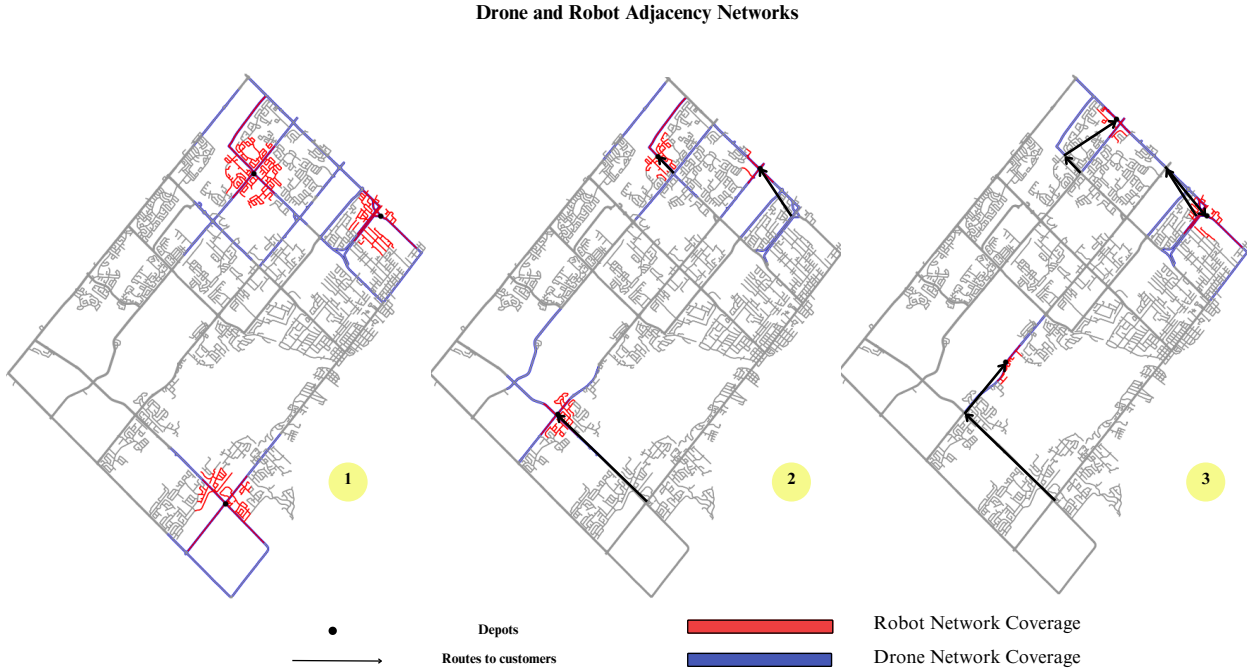


Figure 8: UAV and ADR network coverage during the delivery service

Next, the problem model is trained using the policy gradient reinforcement learning method. More detail is provided in Appendix C.

4.3. Coalitional Vehicle Routing Game

In this section, we develop a coalition game formulation for an E-CPDPTW involving two modes of delivery, i.e., UAVs and ADRs. These agents differ in terms of speed and carrying, as well as battery capacity, and the goal is to allocate the rewards based on their contribution towards completing delivery tasks efficiently within time windows. We consider a set of delivery agents $M = \{D_1, D_2, \dots, D_m, R_1, R_2, \dots, R_n\}$ consisting of m UAVs and n ADRs, where:

- D_i : UAV i with speed v_{d_i} and capacity Q_{d_i}
- R_j : ADR j with speed v_{r_j} and capacity Q_{r_j}

We are given a set of delivery requests $N = \{1, 2, \dots, k\}$, each defined by:

- Pickup node p_r and delivery node d_r for request r
- Time windows $[e_r, l_r]$ for pickup and delivery, respectively
- Demand q_r

The goal is to find optimal coalitional routes for all agent's coalitions such that all requests are fulfilled within their time windows and the total game cost is minimized so that no coalition cost is less than the cooperative cost. At the beginning, a characteristic function is defined for any coalition as a cost of delivery and waiting time such that $C : 2^N \mapsto \mathbb{R}$ associates with each coalition $S \subseteq N$ a real-valued cost $C(S)$, with the assumption of $C(\emptyset) = 0$. Hence, the Equation 22 can be considered.

$$C^{opt}(S) \leq C^R(S) \quad (22)$$

Where $C^R(S)$ is the value for cost as the solution for the E-CPDPTW from reinforcement learning problem as an upper limit for the optimal cost. For two modes of coalitions $S_1 \subseteq N$ and $S_2 \subseteq N$, each of which can particularly be used for specific case of delivery, a set of feasible routing node decisions $x_{S_1}, x_{S_2} \in P$, the nodes (x_{S_1}, x_{S_2}) comprises routing plans x_{S_1} and x_{S_2} is feasible in the routing problem for the joint coalition of modes $S_1 \cup S_2$, that is $(x_{S_1}, x_{S_2}) \in P$, which the customers they are serving is total number of customers in the problem, then it is clear that the following Equation, 23 holds

$$C^{opt}(S_1 \cup S_2) \leq C^{opt}(S_1) + C^{opt}(S_2) \quad (23)$$

Afterwards, using Equation 22 for each coalition, the sub-additive property of the cooperative coalition will hold as Equation 24

$$C^{opt}(S_1 \cup S_2) \leq C^R(S_1) + C^R(S_2), S_1 \subseteq N, S_2 \subseteq N, S_1 \cap S_2 = \emptyset \quad (24)$$

Finally, in order to establish such a core coalition, for any coalition with the conditions of Equation 24, the cost of each coalition mode will be found from Equation 25

$$C(S) = \min \left\{ \min_{S_1 \cup S_2 \subseteq S} \{C(S_1) + C(S_2)\}, C^R(S) \right\} \quad (25)$$

In this regard, for the standard core game theory, the following theorems must hold

Theorem 1. *The cooperative capacitated pickup and delivery game with a time window is sub-additive.*

According to Roger et al. (1991), the core of a game is defined as all allocation costs that are individually rational, fairly distributed, and collectively rational. To find such an allocation, the Equations 26 and 27 must exist. An allocation S is said to be in the core of the game for $S \subseteq N$ if S , which is feasible for N , and no coalition can improve upon it.

$$\sum_{i \in N} C(S_i) = C(N) \quad (26)$$

$$\sum_{i \in S} C(S_i) \geq C(S) \quad \forall S \subseteq N \quad (27)$$

As a result, If a feasible allocation S is not in the core, then some coalition S would exist such that the players in S could all do strictly better than cooperating together and dividing the worth $C(S)$ among themselves.

Theorem 2. *The core game of the CPDPTW game can be empty.*

This case can be held if one of the efficiency, Equation 26 or coalitional rationality, Equation 27, is found with non-feasible allocation. In Shapley (1967), it has been shown by using Linear Programming (LP) that the core game can fall into a situation of not fairly allocating the cost among individuals; thereby, the shared cost to each agent is more than if that agent would have been worked itself.

As proof, a toy example of three customers and three vehicles, one for ADR and the rest for UAV mode, are considered given their travel and waiting cost as well as their features, which may constrain the delivery, such as capacity. As seen from Figure 9, there is one depot from which vehicles begin routing; each request comes with a tuple of q, e, l as demand, pickup window, and delivery window, respectively. Additionally, each vehicle has the unique characteristics of v, Q as their travel speed and capacity. The speed of the ADR and UAV are assumed to be 1 and 3 units, respectively. Also, the capacities of the UAV and ADR are 10 and 5 units, respectively. In this example, we assume that the battery can accommodate travel and that vehicles move constantly. The waiting cost is the same for each mode, whereas the travel cost differs due to the speed. Also, the travelling cost would not be changed in contrast to the waiting time, given the request to be served in the order. This is a simplified version since it can be sufficiently complex due to many possibilities for routing decisions. In what follows, two special delivery cases will be considered to verify the coalition game theorems. This setup's location and time window information can be found in Table 2, with unit dimension. The depot location is at the center of the origin.

Table 2: Toy example input data

Customer	Pickup Location	Delivery Location	Time Window $[e_i, l_i]$	Demand d_i
A	(1, 2)	(4, 5)	[3, 10]	4.0
B	(2, 1)	(5, 3)	[5, 12]	1.0
C	(3, 4)	(6, 2)	[5, 13]	2.5

The cost function C for an agent (ADR or UAV) servicing customers in N is $C = \sum_{i \in N} (t_i^{\text{travel}} + \beta \cdot \delta_i)$ where, t_i^{travel} is the travel time to service customer i and $\delta_i = \max(0, t_i - l_i)$ represents the delay time for customer i , with penalty weight $\beta = 5$ units per delay time unit. Also, t and T show travel and arrival times, respectively.

4.3.1. Sub-additivity Property

The game is sub-additive if working together (ADR and UAV) yields a lower total cost than working separately. By the assumption of $q_i < Q_D, Q_R \forall i \in N$, although $q_i + q_j > Q_D \forall (i, j) \in N, i \neq j$. This condition is true for just one UAV, and the other can simultaneously take at most two delivery requests. Therefore, the cost of travel time for a ADR can be derived by the time it takes to visit all nodes and update the time step accordingly compared with the time window.

ADR. One sub-optimal solution for a ADR is in the order of $P_A \rightarrow P_B \rightarrow D_A \rightarrow P_C \rightarrow D_B \rightarrow D_C$ the cost for each leg of the delivery is $t_A^R = T_A^R = 8.12 \rightarrow$ Within Time Window: $\Rightarrow \delta_A = 0.$, $t_B^R = 11.77 \rightarrow$ Within Time Window: $T_B^R = 11.77 \Rightarrow \delta_B = 0.$, and $t_C^R = 13.18 \rightarrow$ Outside Time Window: $T_C^R = 13.18 \Rightarrow \delta_C = 5.9$. As a result, the total cost for an ADR alone is $C^R = 14.08$.

UAV. The same for each UAV which will obtain the cost for each leg of the delivery is $t_A^{D1} = T_A^{D1} = 2.16 \rightarrow$ Within Time Window: $\Rightarrow \delta_A = 0.$, $t_B^{D1} = 2.69 \rightarrow$ Within Time Window: $\Rightarrow \delta_B = 0$, and $t_C^{D1} = 1.95 \rightarrow$ Within Time Window: $\Rightarrow \delta_C = 0$. As a result, the total cost for the first UAV alone is $C^{D1} = 6.80$. The cost for the other UAV would be such that the orders of A, B are being delivered and then

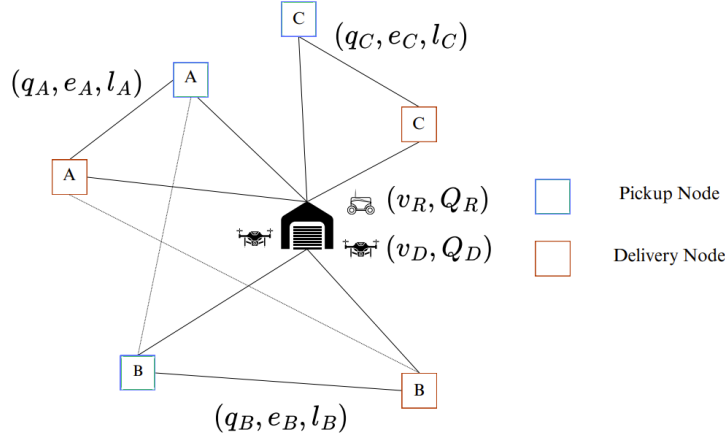


Figure 9: A toy example of CPDPTW with coloured squares as pickup and delivery nodes, as customers with their demand and time windows, and the arcs correspond to the travelling distance

request C . Therefore, $t_{AB}^{D_2} = T_{AB}^{D_2} = 3.46$, \rightarrow Within Time Window: $\Rightarrow \delta_{AB} = 0$, which denotes the cost of having A and B being done. $t_C^{D_2} = 1.95 \rightarrow$ Within Time Window: $\Rightarrow \delta_C = 0$. As a result, the total cost for the second UAV alone is $C^{D_2} = 5.41$.

Working Separately. Put together this total cost when working separately, is $C^R + C^{D_1} + C^{D_2} = 26.29$

Working Together (Coalition). The first UAV will handle A , the second one C , and the ADR will handle B . In this case, the coalition cost can be found by previous computations as $C_B^R = 5.81$, $C_A^{D_1} = 2.16$, and $C_C^{D_2} = 5.41$. Thereby, the cooperative cost is $C^{R,C_1,C_2} = 13.38$. Since $C_{R \cup D_1 \cup D_2} < C_R + C_{D_1} + C_{D_2}$, the game is sub-additive. The cooperative cost is not only less than the sum of the individual cost; their contribution is equal to or less than the previous share.

4.3.2. Empty Core

A coalition can be formed that does not follow the core properties, and thereby, the cooperative performance is not superior, and the individual coalition is preferred. Consider a coalition of the ADR with a group of UAVs, $S \in R, D_1, D_2$. In contrast to each agent coalition, this example is a mode coalition, so it groups each mode separately. The ADR takes the same cost share if working, although UAVs will complete routing as follows.

UAV D_1 goes to customer C , and UAV D_2 takes care of the other customers. As per previous calculations, the cost for this group is $C^{D_1,D_2} = 2.87 + 3.46 = 6.33$. Therefore, when working separately, the total cost, including the ADR, is $C^R + C^{D_1,D_2} = 20.04$. On the other hand, the total cost when these groups work together is again more than in the cooperative case; however, the average cost contribution of UAVs would be more if they work separately, such that $C^{D_1,D_2}/m \geq C^{D_1}$. This would put more load on the first UAV, though it is beneficial for the second UAV. Nevertheless, this is sufficient to ensure that a coalition of two UAVs and one ADR core does not exist.

5. Results

This section conducts extensive experiments on two synthetic and real-world datasets, different request sizes, vehicles, and depots. All simulations are carried out with PyTorch on NVidia A100 GPU.

5.1. Experimental Setup

Node locations are drawn uniformly from the square area of $[0, 5]km$, and the pickup time window of nodes is driven by Poisson distribution for the evening peak hour, in addition to a random delivery time window from $[30, 60]min$ based on the node. The maximum speed of the vehicles is set at $20m/s$ and $8.3m/s$ for UAVs and ADRs, respectively, though they will adjust their speed based on the horizon time window to arrive at the destination on time. The demand volume of a pickup node d_i is uniformly sampled from $(1,10)$, the capacity limit of each vehicle is 5 and 10, and the maximum battery energy for each mode is set as $6.5KJ$ and $4.5KJ$ for UAV and ADR, respectively. The service time at each node is uniformly generated with a scale of two minutes, and the recharging time at each charging station can be up to 10 and 20 minutes. Also, the speed of either of the vehicles visiting the depot for recharging is half of the max speed. The lower limit threshold for the battery is 30% and 20% for UAVs and ADRs, respectively, since they can manage energy while going back to depots. We assume a higher technology readiness level in some parameters, such as battery recharging efficiency. The penalty monetary coefficients for utilizing the UAV and ADR are set separately as $\alpha_1 = 0.6$ and $\alpha_2 = 0.1$ monetary units per minute. According to Sudbury and Hutchinson (2016) and Fortune (2023), these factors are considered as the cost of automated vehicles' utilization for delivery companies. We assume that these vehicles are rented for the peak hours of operation. The pickup time window is set as a hard constraint, and if the vehicle arrives earlier than the pickup time window, it will be penalized as if extra time for the operation in the reward function since the order is not ready yet to be picked up; the cost penalty rate will be ($\alpha_3 = 0.01$). On the other hand, the delivery time window is designed flexibly to encourage vehicles to arrive as soon as possible. If it arrives earlier than the time window, the cost function is set as consistent. Nonetheless, the penalty factor for time delay is $\alpha_3 = 0.05$, the monetary unit per minute delay. More specifically, the delay penalty in case of arriving after the time window is 0.05, meaning compensation for the customers' time, and the delay penalty for arriving before the pickup time window is 0.01 in the case of extra operational costs. Note that if the vehicle arrives before the delivery time window, there would be no penalty since it could arrive within a time window. Furthermore, we set a negative penalty value in the cost function if the battery constraint is violated and falls below the threshold. This factor is considered if there would be another delivery for that unfinished delivery customer; thereby, the battery penalty factor is $\lambda = 1$.

We also present the comparison study between the proposed methodology with state-of-the-art methods, including Google OR Tools and some available state-of-the-art methods, with the general attention model (AM), described as follows.

1. **Google OR-Tools**, a commonly used software for solving vehicle routing problems. For a Python version, we implement the algorithm to solve the E-CPDPTW, which suits our problem constraints with a limit of 3600 seconds.
2. **Gurobi Optimizer**, a mathematical optimization software for solving mixed-integer linear and quadratic optimization problems. We adopt it and modify it for E-CPDPTW and the upper limit of solution time as 3,600 seconds
3. **Attention model (AM)** Kool et al. (2018), the original transformer structure utilizes both the encoder and decoder for vehicle routing. We manually use conventional multi-head attention for the encoder in our setting combined with the our masking scheme in the decoder, ensuring the output solutions and battery constraints for the depot attention layer are feasible.
4. **Heterogeneous AM** Li et al. (2021), heterogeneous attention model for the PDP, in which seven types of attention layers were designed to consider different roles played by nodes while considering the precedence constraint. Their architecture have been incorporated in the encoder augmented with our masking scheme likewise the previous method.

5.2. Policy Network Training

In evaluating both datasets and neural network parameter trade-offs, we construct experiments with three scales, $2N = 20, 50, 120$, and accordingly fix the agent amount with 2, 4, 6, and 10 vehicles. For clarity, we will use the problem name in the following manner. For example, “E-CPDPTW20-d2” indicates the delivery problem of 20 requests with two depot stations. The networks are trained via Adam optimizer with four layers of convolution and eight heads, the node and edge hidden embedding dimension as 128 and 16 respectively, and learning rate $l_r = 0.00005$. We apply greedy decoding for baseline to reduce the reward variance in the back-propagation phase and evaluate the actor parameters in the training process with sampling decoding. The training is done for the cost of 100 epochs, and in each epoch, 2500 batches with 512. The training times for the following cases, 20-1d one vehicle each, 50-3d two vehicles each, and 120-3d three vehicles each, are 21 min, 55 min, and 112 min per epoch, respectively. The training curve for our proposed learning architecture decoding with 20 requests is shown in Figure 10. The average cumulative total cost or denting as total cost versus a number of epochs is depicted. Note that three different assignment methods have been shown: decoding, where both modes are accounted as a pair to pick the highest probability of node for all the agents, and another two decoding assignments, where one of the modes comes into priority. By priority, we explicitly mean picking the highest node assignment probability for any mode comes first. The former is called Paired-RL, and the latter is called UAV-Prior-RL and ADR-Prior-RL, which separately give the fixed assignment order to one mode. To be more specific, the paired-learning decoding would encompass a broader solution space to be explored yet required for the multi-agent policy network training curve to be smoother and less noisy. Otherwise, limiting the decisions for either of the modes might cause agents to receive a high variance in reward. In this regard, we add an entropy regularization term with decaying weight to the loss function to reduce over-fitting.

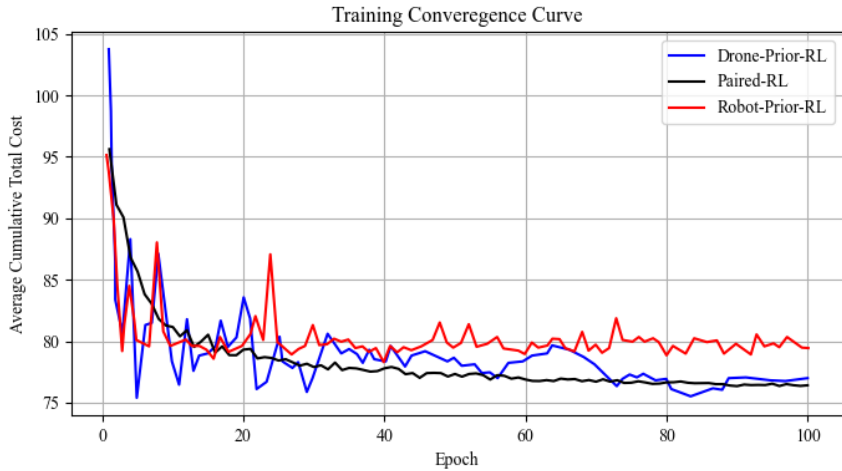


Figure 10: Training convergence curve in 100 epoch

It can be observed by the training convergence curves that the Paired decoding learning shows a stable average cost over time and quickly converges to a 2% cost gap at epoch 40. This is due to the model’s ability to allocate tasks based on the optimal agent for each request, leading to optimal choice over the training process. UAV-Prior also shows efficient behaviour by decreasing the cost significantly at earlier epochs, being able to adapt to the environment; however, the curve is under fluctuations, possibly due to the UAV’s sensitivity to specific conditions like different edge embedding and weather in every batch, which can impact its performance consistency. On the other hand, ADR-Prior shows less variance domain throughout

the training with slower convergence and higher average reward. This can be explained by the fact that, whereas in the UAV-Prior, this decoding struggles to match the efficiency of UAVs in certain scenarios, such as longer distances or time-sensitive demands. Therefore, it can limit the exploration space. In the end, given the performance quality and stability, Paired learning acquires a better solution.

Moreover, the dataset carries the stochastic wind model distribution by Johnson (1985). It substantially impacts the cost function since it can work either in favour of the UAVs or adversely impact when the direction is on the opposite side of the UAV’s speed. Besides, UAV capacity is lower than that of ADRs and carrying heavier payloads will use more power for the same delivery; thereby, training on a variety of datasets and their influence on the cost function, we expect that heavier payload in short distances will be mainly assigned to ADRs and UAVs deliver the far requests, as well the requests which fall in the unfavorable-wind locations for UAVs, will be done by ADRs. However, to avoid over-fitting and trapping in the sub-optimal space, we consider two main wind directions, eastward and westward, to perturb the UAV power consumption model. Otherwise, the reward distribution would be noisy and convergence under such criteria is not guaranteed. Also, we allow the agents to reach a negative battery level and instead add a term to the cost function for a penalty. Otherwise, the action space would be limited, and exploring the optimal solution through the learning process would be difficult.

5.3. Results Analysis

The comparison results of the overall performance are shown in Table 3. The total cost, the gap of each method, and the time spent during inference with three different customer scales are reported, and the optimal solution is considered the minimum cost function. Accordingly, gap denotes the average optimal gap between a result and the baseline solution, written in Equation 28. The number of validation instances is 10000. Besides sampling decoding, another test is denoted as E-CPDPTW(1280), where the decoder samples 1280 times at each step to obtain multiple solutions and selects the solution with the highest reward as the routing solution.

$$\text{Gap} = \frac{1}{N_{\text{test}}} \sum_{i=1}^{N_{\text{test}}} \frac{L(\hat{\pi} | s) - L(\pi | s)}{L(\pi | s)} \quad (28)$$

Table 3: Costs and computing time for E-CPDPTW

Vehicles	Method	E-CPDPTW20-d1			E-CPDPTW50-d2			E-CPDPTW100-d3		
		Cost	Gap, %	Time (s)	Cost	Gap, %	Time (s)	Cost	Gap, %	Time (s)
2	Gurobi	81.15	6.18	7.43	-	-	-	-	-	-
	OR-Tools	89.55	17.17	5.91	-	-	-	-	-	-
	Heterogeneous AM	79.96	4.61	0.33	180.01	3.98	0.73	512.69	8.49	1.38
	AM (greedy)	84.05	9.98	0.21	185.70	7.24	0.80	532.74	12.74	1.52
	E-CPDPTW (greedy)	78.11	2.20	0.58	176.82	2.13	1.32	480.08	1.59	2.45
	E-CPDPTW (1280)	76.43	0.00	0.86	173.13	0.00	1.71	472.56	0.00	3.17
4	OR-Tools	57.04	19.06	12.64	-	-	-	-	-	-
	Heterogeneous AM	49.19	2.67	0.42	65.78	4.90	0.83	321.58	18.38	1.47
	AM (greedy)	51.23	6.93	0.59	58.90	39.17	0.78	314.54	13.10	1.13
	E-CPDPTW (greedy)	50.68	5.78	0.64	103.14	6.54	0.98	287.03	5.64	2.75
	E-CPDPTW (1280)	47.91	0.00	1.05	96.82	0.00	1.06	271.61	0.00	3.16
6	OR-Tools	47.44	24.94	22.92	-	-	-	-	-	-
	Heterogeneous AM	40.85	7.57	0.62	78.14	17.76	0.81	167.39	9.79	1.96
	AM (greedy)	41.02	8.02	0.53	83.73	26.17	0.96	181.28	16.09	1.72
	E-CPDPTW (greedy)	40.60	6.91	0.87	70.79	6.69	1.84	153.36	0.80	2.80
	E-CPDPTW (12800)	37.98	0.00	1.15	66.35	0.00	2.42	152.13	0.00	3.43

Regarding solution quality, our model outperforms classical methods and, in most cases, transformer-based methods. The computation time increases exponentially as the problem scale increases for the exact solvers of Gurobi and OR Tools, which fail to solve instances with > 50 customers within an acceptable time, as well as failure to address constraints to find the optimal solution, which cannot complete the delivery request set. Our model, on the other hand, incorporates operational constraints, which add layers of complexity to the routing problem, and the learning process is accounted for by two different network setups, which again impose more parameters to train, especially for discontinuous reward function, which can lead to unstable learning signals. Thus, we use graph pruning by time-based network adjacency to mask the irrelevant part of the graph and reduce the computational burden. Furthermore, the time window adjacency controls the UAV delivery stage to adapt their speed or travel with the maximum velocity unless returning to the depot. Considering the spatial-temporal information, our dynamic transformer performs significantly better due to the novel exclusive encoder-decoder design to distinguish between each mode assignment and cooperation tasks. Moreover, this model is designed to capture the hard and soft constraints and variety of heterogeneity of different datasets. Therefore, high representation and embedding dimensions and training parameters must be defined to handle such restrictions and capture unpredictable and irregular patterns of on-demand delivery. Nevertheless, considering addressing such operational constraints to this extent, it still can compete with most modern algorithms at the same scale in comparable times. In addition, the training curve has been examined to determine if the decoding strategy would differ based on the paired and fixed cooperative priority-based assignment of the modes to the customers.

5.4. Robustness Test

The framework for a multi-modal delivery system has been designed to address issues with the delivery system in urban environments. However, it is appealing to incorporate issues from customer perspectives to establish a robust performance. Therefore, it is crucial that our model produces reasonable results for cases that come with uncertainty or undergo more realistic application, leading to a sustainable level of service.

First, to ensure the adaptability of the proposed model to real-world scenarios, a few layers of uncertainty will be added to both the spatial and temporal aspects of delivery requests, such as non-uniform customer locations, tighter time windows, and directed wind conditions. Second, by enhancing the functionality of this study to a broader application, the practical implications are expanded to critical cases of deliveries, such as medicine deliveries, where there is an urge for the parcels to be delivered on time.

The application of our trained models in real-world scenarios is described, where depot and delivery locations are simulated within real-world road networks retrieved from OpenStreetMap for the city of Mississauga. In this regard, these scenarios will verify how the multi-agent reinforcement learning model robustness performs in different wind situations and spatial-temporal patterns of order arrival. This will facilitate comprehending various circumstances that affect the model’s capacity to produce effective routing options. We make different scenarios where the test dataset is not uniformly distributed in the case study; the pickup and delivery locations are distributed based on non-uniform distribution for scattered places, as well as a case of tightened time window. Furthermore, the wind has a constant direction over the case study, such as Eastward and Westward, to evaluate how it would affect each mode’s assignment pattern, given that UAVs can either benefit from the wind direction or be confined due to more battery usage. The wind speed magnitude can be up to $12m/s$.

Like the previous analysis, Table 4 demonstrates a performance for different scenarios, their cost, gap, and computation time for a fleet of both three vehicles for each mode. It is noted that the analysis is conducted only for transformer-based methods since the traditional approaches were not superior in the last section. Also, for the constrained Gurobi and OR Tools, a soft penalty term is added to the cost function, which makes the agents leave the task unfinished and not visit nodes in the right order, making it complex

Table 4: Costs and computing time for E-CPDPTW with non-uniform dataset

Case	Method	E-CPDPTW20-d1			E-CPDPTW50-d1			E-CPDPTW120-d2		
		Cost	Gap, %	Time (s)	Cost	Gap, %	Time (s)	Cost	Gap, %	Time (s)
Eastward wind	Heterogeneous AM	38.51	15.10	0.74	76.51	12.67	0.84	170.68	11.55	1.76
	AM (greedy)	39.92	19.34	0.71	78.24	15.20	0.73	192.23	25.58	1.82
	E-CPDPTW (greedy)	35.80	6.99	0.93	69.57	2.43	1.76	158.41	3.52	1.63
	E-CPDPTW (1280)	33.46	0.00	1.02	67.92	0.00	1.92	153.03	0.00	3.42
Westward wind	Heterogeneous AM	40.31	22.89	0.77	77.97	17.16	0.81	168.31	11.96	1.52
	AM (greedy)	41.74	27.33	0.70	75.04	12.75	0.83	185.60	23.43	1.74
	E-CPDPTW (greedy)	34.11	4.02	0.88	69.33	4.16	1.48	155.09	3.16	1.66
	E-CPDPTW (1280)	32.79	0.00	1.13	66.56	0.00	1.73	150.35	0.00	2.89
Tight time window	Heterogeneous AM	43.16	11.20	0.80	82.12	8.26	0.95	207.06	24.20	1.68
	AM (greedy)	44.43	14.43	0.75	81.90	8.00	0.70	216.25	29.78	2.15
	E-CPDPTW (greedy)	42.55	9.61	0.94	77.81	2.59	1.88	168.22	1.17	1.85
	E-CPDPTW (1280)	38.82	0.00	1.21	75.85	0.00	1.91	166.63	0.00	3.71

to find the optimal solution. The results show that heterogeneous attention mechanisms can handle these variations better due to their inherent capabilities in managing data inputs and variable constraints rather than the original transformer model. Moreover, our model executes in a comparable running time, though it is considerably more robust than the regular situation. This led to the advantage of our model over the other models in terms of model specification and the power of incorporation of graph attention network in capturing inter-nodal information, as well as how our novel approach can produce high-quality solutions. The cost value, however, does not always increase in the case of uncertainty. For example, in the case of eastward wind and $n = 20$, the cost is reduced, and for $n = 50$, it is increased to some point. The reason for such behaviour is that the wind may influence the ADR adversely, leading to higher battery consumption. Also, it can take place as it assists the UAV in moving downstream airflow, which is in the same direction. Both windy cases suggested that the approach finds optimal solutions as it conducts graph data processing much more efficiently yet with more computation effort. Additionally, the tight time-window case is when the difference between pickups and deliveries is up to 25 minutes (about 20% tightened), showing the variation of the solution under such modification. It can be seen that presumably, for shorter time windows, the model will not be effective, and also, the result alteration is more significant when it comes to smaller networks, most probably due to the lack of sufficiently large customer nodes so it can counter-effect wind influence and time window distribution.

Furthermore, to draw the patterns of spatial-temporal requests and how the assignment of multi-modal delivery in the presence of wind can be done, for each case, the assignment map for both modes is represented in Figure 11. The deviation from the no wind case is noticeable, where UAVs tend to take the wind-ward delivery action. For the tight time window case, battery limit constraint has been treated less strictly due to some cases that might have appeared with long distance from the depot, making it less efficient for the electric delivery. Both modes can mainly do one delivery at a time in such situations. In contrast, with a uniform test set, they can conduct multiple deliveries and even visit the depot during the travel. However, the system’s overall performance is comparably acceptable due to changing conditions in real-time and assigning UAVs to the opposite side of delivery to move in favour of the wind.

Moreover, rigorous training criteria have been set to consolidate the desired level of service in time-critical delivery applications when the time delay is with more linear penalties accounted for different delivery cases. It has been assumed that the delay penalty is highest in the case of an emergency when customers, in fact, are patients in the medical centers awaiting an organ for surgery or transplant. Another case is assumed to be of priority but not as critical as the first one, medicine delivery for hospitals or customers.

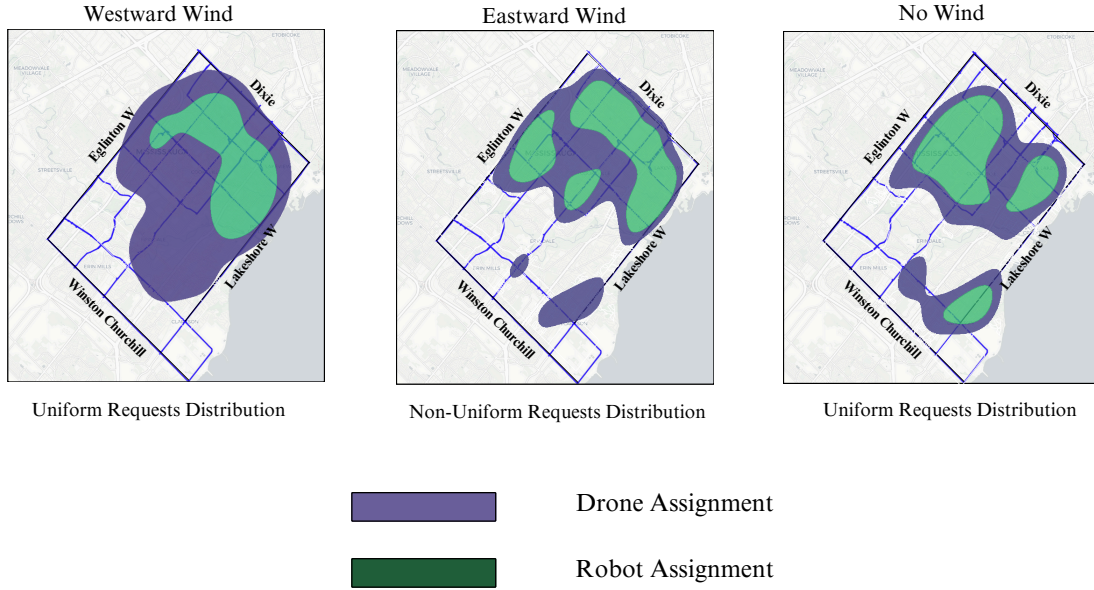


Figure 11: Multi-modal assignment distribution in the existence of uncertain conditions

The penalty for obtaining this learning curve is set as $\alpha_3 = 0.1$, and, for the former, is set as a higher rate, $\alpha_3 = 0.2$, which reinforces the time-sensitive delivery. In addition, the rate of delay penalty when vehicles arrive earlier than the pickup time window is set as 0.01 to enforce agents to avoid sub-optimal solutions. Finally, the baseline training curve for a guaranteed service level is considered a typical parcel or meal delivery, though with a stricter penalty on battery violation and increasing the battery threshold by 20%, ensuring a vehicle would not fail during the delivery. The output of these scenarios is depicted in Figure 12. According to the Figure, emergency and medicine delivery both result in a higher overall cost and drop drastically from the initial point where the weights of the training parameters are randomly generated, leading to the initial cost being high, and after a few epochs, they can manage to converge; however, it cannot improve the policy much further due to higher prioritization to delay penalty and remain in the local minima. This behaviour can be explained by agents increasing travel costs to ensure no battery and time delay violation happens. On the other hand, the parcel delivery case does not give much importance to the time delay, leading to the model learning to find a balance of battery usage with delay penalties to avoid delivery failures despite the fluctuation, which is mainly because of incurring variance reward due to battery constraint, the training curve can converge and perform more stable than other cases. Nevertheless, our model can train priority-based, time-sensitive delivery, focusing on cost-efficient routes, achieving low time delay and fast convergence, which is crucial for optimizing multi-agent in urban environments.

5.5. Cooperative Coalition Delivery

This section analyzes the cooperation potential of the multi-modal system in the context of urban on-demand delivery. Given the complex nature of such an environment and various autonomous vehicle capabilities, it is best to use the most effective combination of UAVs and sidewalk ADRs. Forming a collaboration framework, stakeholders can be encouraged to pool their vehicles, leading to flexible coverage for

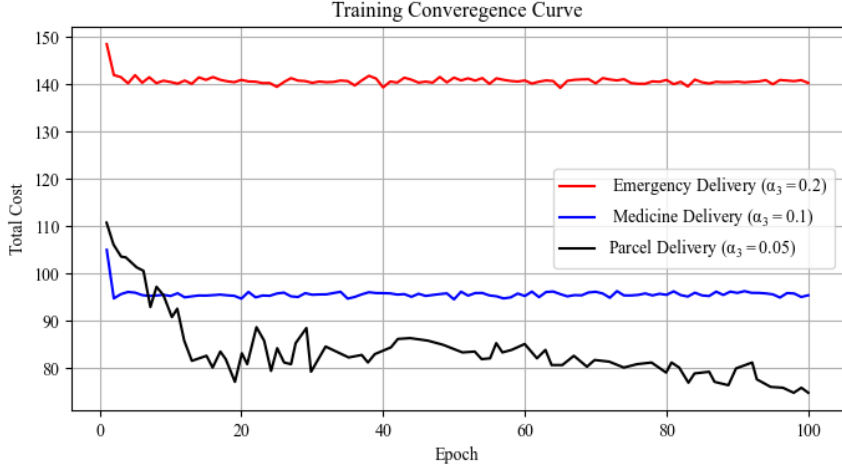


Figure 12: The learning curve for the various delivery cases from low to high critical

fluctuating demand, reducing operational costs, and more efficient delivery in a cooperative manner. First, based on the coalition game theory, the existence of such optimal cooperation must be verified, and cost allocation will be shared after the redistribution of the cost accordingly. Next, the advantages of cooperative delivery operations can be assessed using this approach, which is how forming coalitions can lead to optimal costs and improve the level of service. Introducing a coalition game-theoretic approach, the ability of cooperative behaviour is evaluated by the Algorithm 1, which leverages a reinforcement learning trained model of E-CPDPTW across ten agents—five UAVs and five ADRs.

We extend this section to conduct a core analysis and obtain a potential cooperative coalition which can be promoted to be incorporated among companies encouraged to decrease their utilization cost and increase the level of service, as well as analyze the algorithm’s generalization along different scales of the problem. The network generalization section is done, followed by coalitional analysis using the high-quality solution extracted by the trained model of generalizing varying among agents.

5.5.1. Coalition Generalizability

To verify the generalization of our method, we investigate three cases, which are depicted in Figure 13. Three different configurations are determined by two parameters of ρ and ζ : the time proximity threshold, keeping the graph as a time adjacency matrix, and the probability of obstacles along each node. First, (a) shows a low connectivity and scattered environment, (b) accounts for medium connection and density of the obstacles, and (c) demonstrates a high-density area with most of the nodes connected. The computation time will increase from the former to the latter scenario owing to the existence of more intermediary nodes, which will do the shortest path computation for the UAVs.

We analyze the trained model’s generalization performance, focusing on its ability to handle problems with different configurations: obstacle density and time-proximity network. Figure 14 demonstrates the generalization result of the problem from 10, 20 and 25 requests on three different network configurations, where the urban environment becomes denser from case (a) to (c) and also becomes fully connected from sparse time-based weighted-graph-network. We have utilized the trained model for each request with the case (b) criteria and applied that to the 1000 test instances to obtain how these models generate solutions for the two other cases.

The problem configuration shows reasonable performance when generalized to fully connected and

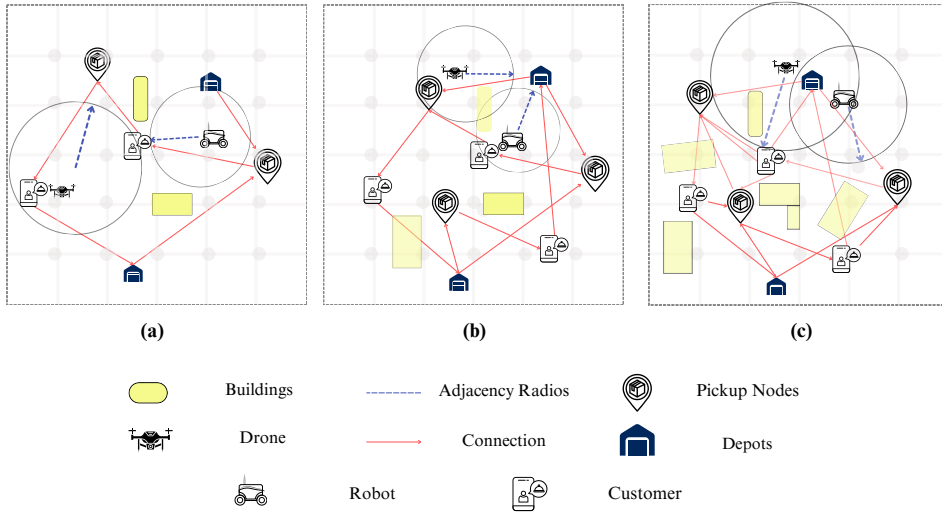


Figure 13: Various graph adjacency network configurations

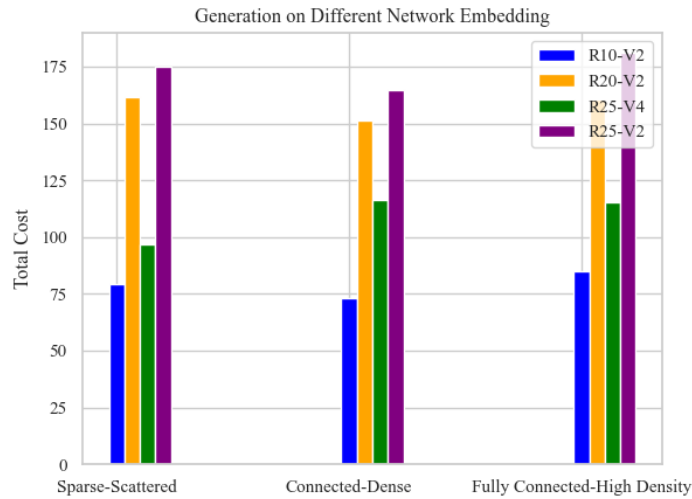


Figure 14: Generation from sparse to fully connected and dense graph network.

high-density cases, as the edge weights are supposed to increase due to a non-existent point-to-point travel path, and UAVs have to use intermediary nodes, thereby higher travel costs. The generalization of the larger case on the smaller case is not expected to work well because of the excessive information carried by the larger case. It takes account of every node connection regardless of their time proximity, which will pose more time for computation on encoding unnecessary datasets sparsified on the lower scale problem. However, even models trained on small-scale problems can achieve comparable results when applied to larger-scale problems, and the cost function will be increased since more graph distance calculations are computed. The core of the performance improvement is due to the nature of the customized graph attention, which gives importance to the time-based graph connectivity encoding, reflecting in the decoding scheme

to output the closest time window node candidates. This has not been addressed in previous studies. One of the advantages of our study is that for larger scale problems, it is not inferior if not outperforms the computation cost of generalization and scalability such that it can be used for any type of urban network delivery since it bypasses the municipality and operational constraint together with incorporating uncertainties. Overall, it can be observed that the cost of sparse-scattered is higher due to higher edge weights from fewer direct connections, which restrict route decision-making flexibility. On the other hand, the fully connected network’s primary advantage lies in flexibility since the increased connectivity does not necessarily mean lower costs, as the model already has efficient routes available in the Connected-Dense setup. As a result, we can conclude that more edge connections do not always lead to better cost estimation, although the weight magnitude from the denser case to the scattered case might not work as efficiently as the scattered to the denser edge-weighted graph.

Besides the internal component of different layouts of urban configuration, the model generalization on different problem scales is worth exploring and, in fact, crucial for the time-saving of using the trained model of the smaller network for larger cases, especially generalizing on a different number of vehicles to verify the effectiveness of the proposed model. The policy learnt from the training is designed independently of the number of agents, incorporating mean-pooling of the agent’s context embedding and the network embedding. To this end, we use the pre-trained models for three scales of 20, 50, and 120 to generate solutions for smaller to larger and larger to smaller networks. Figure 15 demonstrates validating the generalized solution in a box plot for all three networks.

Algorithm 1 Core Coalition for E-CPDPTW with UAVs and ADRs

- 1: **Initialization:** Trained RL actor model for ten agents, $C(N) \simeq C^{opt}(D, R)$, $\forall D \subseteq N^d$ and $R \subseteq N^r$ for the coalition
- 2: **Input:** Initialize D and R for generalized trained model $C(S) = C^{opt}(D, R)$ for any coalition $S \subseteq N^d \cup N^r$
- 3: Define efficiency condition $C(N)$ for grand coalition N (all agents) such that: $\sum_{i \in N} C(S_i) = C(N)$
- 4: Define coalition rationality condition: For any subset $S \subseteq N$: $\sum_{i \in S} C(S_i) \leq C(S)$

Step 1: Solve for Cost of Individual Coalitions

- 5: Compute cost $C(D)$ for D UAVs of E-CPDPTW
- 6: Compute cost $C(R)$ for R ADRs of E-CPDPTW
- 7: Compute cost $C(D + R)$ for D UAVs and R ADRs working together of E-CPDPTW

Step 2: Check Sub-additivity Condition

- 8: **if:** $C(D + R) \leq C(D) + C(R)$
- 9: The game is sub-additive (cooperation reduces cost)
- 10: **else:**
- 11: The game is not sub-additive
- 12: **end**

Step 3: Efficiency and Coalition Rationality Conditions

- 13: Set $C(S_i)$ as the cost share allocated to each agent in D UAVs and R ADRs
 - 14: **for** each coalition $S \subseteq N$:
 - 15: **if:** $\sum_{i \in S} C(S_i) > C(S)$ for any coalition S :
 - 16: The core is empty
 - 17: **elif:** $\sum_{i \in N} C(S_i) = C(N)$ is satisfied for all $C(S_i)$
 - 18: The core is non-empty
 - 19: **end**
 - 20: **end**
-

The overall result shows an acceptable solution generated from each of the scales to others; most notably, the generalizing on smaller networks from the trained model of larger networks produces better results. This

Generalization Performance of E-CPDPTW

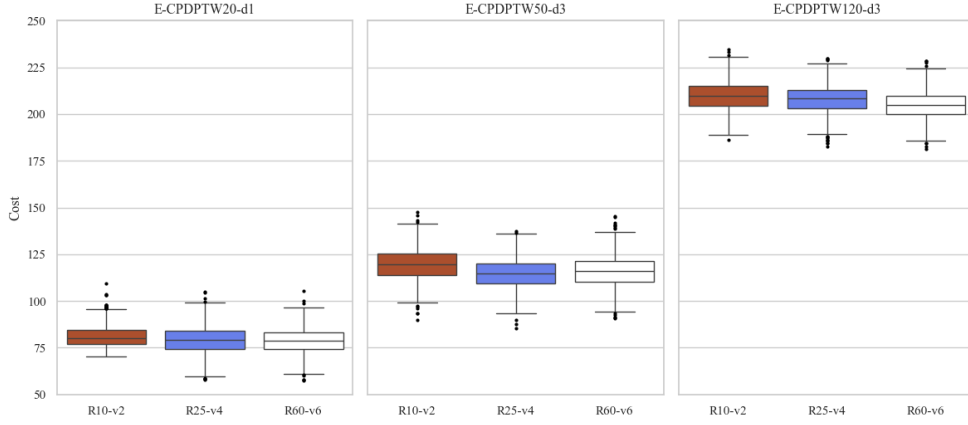


Figure 15: Generalizing on different problem scales.

is probably due to the inclusion of smaller and more information on the network embedding. This variation can also be explained by the different number of depots in each case, which causes the training parameter not to capture the depots embedding well. In addition, as the scale of the problem gets larger, generalization results undergo variability, particularly due to managing the fewer vehicles within the larger network and generalizing from lower vehicle-to-request ratio distribution, which causes ineffectiveness in high request densities assignment with limited resources. Nevertheless, in the constant size of the graph, the model’s ability to generalize is still effective, and in the next part, we analyzed the core game theory for the constant size of the network, yet various number of agents.

5.5.2. Coalitional Ability

We use the pre-trained model for E-CPDPTW120-d3 for ten agents (five of each mode) to conduct a test to find the core coalition among the subset of agents. To evaluate the cost function for each coalition, we use the generalizing on the pre-trained model to obtain cost values to avoid the high computation expense of training for each coalition. The coalitions are of the two separate modes of ADRs ($r \in \{1, \dots, N^r\}$) and UAVs ($d \in \{1, \dots, N^d\}$) set, assumed to have no intersection; thereby, we would then consider a convex game according to Shapley (1971). This refers to Equation 29, a property of convex game for coalitions formed of cooperation.

$$C(S_1 \cup S_2) \leq C(S_1) + C(S_2) - C(S_1 \cap S_2) \quad \forall S_1, S_2 \subseteq N \quad (29)$$

Since the formation is under two completely different coalitions, we conclude that $S_1 \cap S_2 = \emptyset$; therefore, the convex property of the game is met. The Algorithm 1 is used here to assess how coalitions will perform and if the core exists. For up to a group of just consisting of either UAVs or ADRs, the individual cost of both modes will be calculated, as well as their coalition. Subsequently, the sub-additivity and efficient conditions are checked so that not only must the cooperative cost be less than both individual modes, but also, the newly allocated cost of the coalition must be less than the average mode cost alone. Figure 16 displays contour plots for coalition gains; the heat map bar shows the difference between the sum of individual and cooperative modes. Note that the spectrum level is set to be sufficiently high to obtain a smooth colour transition graph. However, it is clear that the core analysis plot is discrete. The star sign in the figure

indicates if the core exists, given its criteria. It was observed in both scales of the problem that the core exists except in the network size of 120, where only one UAV is operating. This can be mainly because in the larger network, having one UAV independently from the ADR numbers cannot accommodate the demand due to high delays in the deliveries of ADRs, yet it is achievable in the $n = 50$. Nonetheless, lower coalition values are observed in both graphs where fewer UAVs are involved, and the lowest value gain is obtained, which fails to perform well in such a large network. It is, however, toward yellowish regions where the most value is gained by acting cooperatively instead, which is increasing where both the number of UAVs and ADRs increase. This implies that a balanced configuration, often considered a homogeneous coalition, leads to stable and cost-effective matching policies. Furthermore, the non-homogeneous formations can also be a feasible and comparatively fair candidate solution for both sub-figures. In fact, most of the coalitions will fit into the core game of E-CPDPTW and deploy at least one UAV in the fleet; the requests are delivered in such a network size, yet not as efficient as operating more ADRs to deal with the high-capacity demands. In other words, in delivery systems, especially in large networks, it is more convenient if one UAV goes to multiple pickup and delivery locations than if one of them is assigned to an ADR if not mandated by capacity constraint violation. Moreover, the battery consumption rate of UAVs is significantly higher than that of ADRs compared to the current state-of-the-art technology, which leads them to visit recharging stations more frequently and puts more load on urban areas' serviceability. Therefore, using coalitions of ground mode, which can keep away from this shortcoming, is of paramount importance, as can be implied from the result of the core analysis.

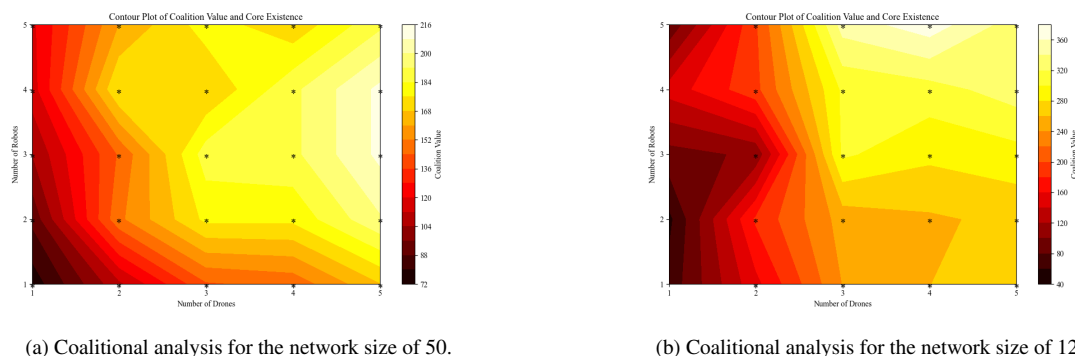


Figure 16: Core coalition counter-plot for five agents in each mode. The sidebar shows the cost difference and denotes the incentives for forming coalitions and working cooperatively.

Finally, according to Figure 16, the optimal coalition for both cases is not when all resources are available; instead, middle regions of the plot, where starting from 3-5 UAVs and 3-5 ADRs, tend to exhibit higher gain. Although it has been inferred that having more vehicles will substantiate the core existence and applicability, it can be achieved in the case of $n = 120$ with only 80% of resources. This is also observable in the case of $n = 50$ when ADRs are of the 80% of resources. Certain scenarios as well such as $r = 4, d = \{2, 3\}$ on the scale of 50 or $r = 3, d = \{1, 2, 3\}$ on the scale of 120, do not support the overall trend of the graph, which tend to gain more values for utilizing more vehicles. The rationale behind this is mainly due to a misfit in the generalization of larger to lower fleets, which causes the graph not to be smooth and continuously changing. However, the explanation for the former statement of maximum utilization gain is believed to be underlying the fact that systems have found that specific coalition to be more optimal given the prioritizing of the sufficient number of UAVs to avoid the high cost. Note that not necessarily adding more vehicles will lead to redundancy, where each additional agent contributes less benefit to the coalition

and may put extra effort into other vehicles and reduce the overall efficiency. As a result, achieving the optimal coalition value depends on finding the right balance between the number of UAVs and ADRs.

6. Conclusions and Future Directions

We present a comprehensive framework for multi-modal autonomous delivery utilizing ADRs and UAVs in urban environments. By addressing critical challenges related to on-demand delivery in high-density areas and efficient vehicle allocation, the proposed framework aims to enhance the accessibility of delivery services while optimizing network infrastructure. Developing an interactive cooperative allocation system ensures a centralized decision-making process to determine the most effective delivery mode regarding efficiency and time delay.

The stochastic nature of the delivery problem is acknowledged, considering factors like unknown demand, airspace regulations, and unpredictable weather conditions. Our solution tailored a deep reinforcement learning approach, specifically the transformer architecture with edge-enhanced attention models, to achieve optimal assignment and routing in urban environments. By simulating the delivery task for the fleet, our methodology accounts for delivery priority, vehicle states, and environmental changes. Moreover, the coalitional game theory model has been adopted to investigate potential cooperative cost profit by which various coalitions are formed. In addition, core properties where they proved to exist have been established to identify multi-modal delivery advantages over uni-modal and cost distribution among groups of vehicles.

Our proposed model exhibits superior performance in urban on-demand delivery systems applied in various delivery scenarios, giving importance from customers' to commercial perspective to accommodate large high-density areas utilizing cooperative operation of UAVs where reducing delay costs and handling time-sensitive deliveries is accomplished and ADRs carrying larger payloads and decrease the burden from the fleet is done. The problem of E-CPDPTW has been investigated in a variety of aspects, including robustness tests of operating uncertain and irregular patterns of time-location distribution as well as wind conditions, which could be potentially utilized in such situations owing to its sustainable performance. In addition, coalition following the generalization ability of such a mode has been analyzed in various configurations, scales, and multiple agents, verifying a robust and scalable model.

There are several future directions where the research can be further developed. Firstly, refinement of the proposed framework will be essential to account for real-time constraints and dynamic adjustments in response to changing environmental conditions, such as congestion in the edge insertion technique. Exploration of additional factors, such as airspace conflict resolution and local regulations, will contribute to a more realistic and adaptable delivery system. Additionally, the system's scalability in the context of multi-agent reinforcement learning warrants investigation. Extending the framework to handle a larger fleet of autonomous vehicles, diverse urban environments of different layouts, and decentralized execution will be crucial for practical implementation and widespread adoption. Furthermore, evaluating the proposed on-demand delivery system under varying external factors, such as vehicle failure and order cancellation, will be a focus of future work. Continuous optimization of the objective function, considering both the level of service and delivery cost, will contribute to an increasingly efficient and resilient autonomous delivery system.

Appendix A. Mixed Integer Programming (MIP) Model for E-CPDPTW

The objectives and constraints in the mathematical formulation are listed as follows. The objective function is shown in the Equation A.1.

$$\min R = \alpha_1 \sum_{k \in N^d} \sum_{(i,j) \in N} t_{ijk} X_{ijk} + \alpha_2 \sum_{k \in N^r} \sum_{(i,j) \in N} t_{ijk} X_{ijk} + \sum_{i \in P \cup D} \alpha_3 |T_{ik} - e_i| + \sum_{i \in P \cup D} \max\{T_{ik} - l_i, 0\} \quad (\text{A.1})$$

Where t_{ijk} is time travelled by vehicle k between node i and j , T_{ik} is the arrival time of the vehicle k at node i , α_1 and α_2 are positive monetary conversion factors pf utilizing UAVs and ADRs respectively per hour. Also, the α_3 is the monetary coefficient of waiting time penalty for customers that the delivery company has to compensate in the case of delayed delivery. The second and third terms can only be positive because of the violation of time constraints. If, in the second term, the vehicle happens to arrive earlier than the specified time window, we treat the time difference loss as the first term of the cost function. Additionally, the equations that constrain this objective function are discussed below.

$$\sum_{j=0}^{P \cup D} X_{ijk} = 1, \forall k \in \{N^r \cup N^d\} \quad \forall i \in C \quad (\text{A.2})$$

$$\sum_{i=0}^{P \cup D} X_{ijk} = 1, \forall k \in \{N^r \cup N^d\} \quad \forall j \in C \quad (\text{A.3})$$

$$\sum_{k=1}^{N^r \cup N^d} \sum_{i=0}^N X_{ijk} = 1, \forall i \in \{P \cup D\} \quad (\text{A.4})$$

$$\sum_{i=0}^{P \cup D} X_{ijk} = \sum_{i=0}^{P \cup D} X_{i(j+n)k}, \forall j \in P, \forall k \in \{N^r \cup N^d\} \quad (\text{A.5})$$

$$T_{ik} \geq e_i, \forall k \in \{N^r \cup N^d\}, \forall i \in \{P \cup D\} \quad (\text{A.6})$$

$$T_{ik} \leq T_{k,i+n}, \forall i \in \{P\}, \forall k \in \{N^r \cup N^d\} \quad (\text{A.7})$$

$$T_{ki} + s_i + t_{ijk} \leq T_{kj} + (1 - M)X_{ijk}, \forall k \in \{N^r \cup N^d\}, \forall (i, j) \in \{P \cup D\} \quad (\text{A.8})$$

$$0 \leq u_i^k \leq Q_k, \forall k \in \{N^r \cup N^d\}, \forall i \in \{P \cup D\} \quad (\text{A.9})$$

$$u_i^k = u_j^k + q_j + (1 - M)X_{ijk}, \forall k \in \{N^r \cup N^d\}, \forall (i, j) \in \{P \cup D\} \quad (\text{A.10})$$

$$e_i^k - e_{ijk} + B^k (1 - X_{ijk}) \geq e_j, \forall k \in \{N^r \cup N^d\}, \forall (i, j) \in \{P \cup D\} \quad (\text{A.11})$$

$$e_{min} \leq e_i^k \leq B^k, k \in \{N^r \cup N^d\}, \forall i \in \{P \cup D\} \quad (\text{A.12})$$

$$e_i^k = B^k, \forall k \in \{N^r \cup N^d\}, i \in C \quad (\text{A.13})$$

$$X_{ijk} \in \{0, 1\}, \forall (i, j) \in \{P \cup D\}, \forall k \in \{N^r \cup N^d\} \quad (\text{A.14})$$

The constraints in Equations A.2 and A.3 ensure the vehicles depart from and return to any depot, whether for recharging or ending the tour. The Equations A.4 and A.5 ensure the requests are only served once and by the same vehicle. The constraints in Equations A.6, A.7, A.8 ensure that vehicles cannot start service at a location earlier than its early time window and cannot be later than the service at its corresponding delivery location, and M is a positive large number. All vehicles must service the pickup location earlier than the delivery node and account for each node's service time, s_i . The capacity constraint of the vehicles and the load balance update is given in Equations A.9 and A.10, with u_i^k denoting the k th vehicle's load after the service at the i th location is done. Equations A.11, A.12, and A.13 denote battery level balance update, capacity constraint, and recharging state after visiting depots, respectively, with e_i^k denoting the k th vehicle's battery level after going to i th location. Lastly, Equation A.14 notes that the binary variable.

Table A.5: Parameters and Definitions

Parameter	Definition
C	Depot instances set
P	Set of pickup nodes
D	Set of Delivery nodes
E^d	Set of UAV's edges network
E^r	Set of ADR's edges network
$[e_i, l_i]$	Early and late time window
q_i	Demand of customer
N^d	Number of UAVs
N^r	Number of ADRs
$N^{d,r}$	Number of vehicles
Q_k	Capacity of vehicle
B_k	Battery level of vehicle
N	Number of customers
T_{ik}	Arrival time of the vehicle k at node i
t_{ijk}	time traveled by vehicle k between node i and j
e_{min}	The minimum battery capacity of vehicle j
X_{ijk}	Binary decision variable for whether the vehicle k travels from vertex i to vertex j

Appendix B. UAV Energy Consumption

UAVs and ADRs are powered by batteries, and due to the limited capacity of the battery charge, they need to recharge their battery once they return to depots. Additionally, there are some factors in the urban area where the power consumption of these electric vehicles is not constantly changing, such as the magnitude and direction of the wind, ground friction, and variable speed of vehicles, which all affect the power consumption. For each vehicle, we use a standard model in previous studies. For UAVs, the model proposed by (Stolaroff et al., 2018) for power consumption is utilized, and we incorporate a stochastic wind with random turbulent flow from (Kimon and George, 2015), where the power consumption is summarized as Equation B.1.

$$P = \frac{T(v_a \sin \alpha + v_i)}{\eta} \quad (\text{B.1})$$

where α is the angle of attack, T is thrust, v_a is the UAV speed, η is power transfer efficiency, and v_i is the induced speed, which can be found by solving Equation B.2.

$$v_i = \frac{g \sum_{k=1}^3 m_k}{2n\rho\varsigma \sqrt{(v_a \cos \alpha)^2 + (v_a \sin \alpha + v_i)^2}} \quad (\text{B.2})$$

where n is the number of rotors, and ς is the area of the spinning blade disc of one rotor. Besides, the angle of attack α and thrust are given by Equation B.3 and B.4, respectively.

$$\alpha = \tan^{-1} \left(\frac{\frac{1}{2}\rho \left(\sum_{k=1}^3 C_{D_k} A_k \right) v_a^2}{g \sum_{k=1}^3 m_k} \right) \quad (\text{B.3})$$

$$T = W + D = g \sum_{k=1}^3 m_k + \frac{1}{2}\rho \sum_{k=1}^3 C_{D_k} A_k v_a^2 \quad (\text{B.4})$$

The first term reflects payload and UAV weight, and the second term is the parasite drag force, with a coefficient of C_{D_k} and the projected area perpendicular to travel A_k for each UAV component. It is noted that the stochastic wind model in Equation B.5 in which a constant wind is combined with a random turbulence flow is incorporated from (Kimon and George, 2015).

$$\begin{aligned} \dot{x} &= v_a \cos \psi + v_w \cos \psi_w \\ \dot{z} &= v_a \sin \psi + v_w \sin \psi_w \end{aligned} \quad (\text{B.5})$$

here v_a and v_w indicate the airspeed and wind speed respectively; $\chi = \tan^{-1}(z/x)$ is the course angle; ψ is the heading angle of the UAV; and ψ_w is the wind course angle. we consider the UAV's velocity to be constant in the course of doing the delivery task; thus, Equation B.6 shows the final corrected velocity.

$$v_a = \sqrt{2v_g^2 + 2v_w^2 - 2v_g v_w \cos(\psi_w - \chi)} \quad (\text{B.6})$$

Furthermore, for the ADR, we use the simple kinematic model and incorporate friction as the only force applied to ADR operation, Equation B.7, where the parameter is followed by (Xiao and Whittaker, 2014).

$$P = C_r(M + m_{pl})gv/\nu \quad (\text{B.7})$$

Where C_r is the friction coefficient, M is the ADR weight, m_{pl} is the payload weight, ν and ν are the velocity and power efficiency, respectively.

Appendix C. Training Algorithm

The policy gradient network is adopted for the training with Adam optimizer (Sutton et al., 1999), which algorithm is shown in Algorithm 2. Since the action space in a routing problem is discrete and expands exponentially as the scale of the problem increases. A policy-based reinforcement method is commonly employed to address this, comprising an actor and a critic network (Li et al., 2021). In this method, the actor-network generates a probability vector over all actions based on the current state at each step and selects an action accordingly. This process iterates until the terminal condition is met. The reward for the actor-network is computed by summing up the cumulative rewards at each step throughout the entire process. Serving as a baseline for the actor-network, the critic network calculates the baseline reward solely based on the initial state to reduce variance. Following the receipt of the rewards from the actor-network and the baseline reward from the critic network, the policy gradient method is applied to update the parameters

of both networks. In this update, the actor-network is trained to discover solutions of higher quality. Critic and rollout baselines are the network for comparison. At each episode, a batch of samples is fed to the RL agent, and by applying a transformer to the instances, the output probability of the decoder generates a candidate sequential node for routing, followed by collecting a reward. Afterwards, the policy gradient estimator will update the parameters θ with a baseline π^B , using Equation C.1.

$$\nabla_{\theta} L(\theta) = \frac{1}{B} \sum_{i=1}^B \left[\frac{1}{N^{d,r}} \sum_{k=1}^{N^{d,r}} (\mathcal{R}(\pi_i) - \mathcal{R}(\pi^B)_k) \nabla_{\theta_k} \log p_{\theta_k}(\pi_i) \right] \quad (\text{C.1})$$

where B and $R(\pi^{BL})$ are the batch size and the baseline reward, respectively. When using a rollout baseline, θ is replaced by the baseline reward at the end of each episode if the test results are significant with confidence of 95%.

Algorithm 2 Policy gradient algorithm

```

1: Input: the number of iterations  $N$ ; iteration size  $I$ ; batch size  $b$ ; number of batches  $B = I/b$  maximum decoding length
    $T$ ; t-test threshold  $\alpha$ 
2: Initialization: initial parameters  $\theta$  for policy network  $\pi_{\theta}$  initial parameters  $\varphi$  for policy network  $\pi_{\varphi}$ 
3: Generate  $A$  E-PDPTW instances randomly
4: for epoch = 1, 2 ...  $N$  do
5:   Calculate the baseline network solution and reward  $R(\pi_{\varphi})$ 
6:   for  $i = 1, 2 \dots B$  do
7:     for  $t = 1, 2 \dots T$  do
8:       Calculate the output action of policy network step  $t, a_t \sim \pi_{\theta}(a_t | s_t)$ 
9:       Observe reward  $r_t$  and next state  $S_{t+1}$ ;
10:    end
11:    Calculate the reward  $R(\pi_{\theta})$ ;
12:    Calculate gradient  $\nabla_{\theta} J(\theta)$ 
13:    Update the parameters;
14:  end
15:  Calculate the value of the t-test  $\varepsilon$ ;
16:  if  $\varepsilon < \alpha$ 
17:    Update baseline network parameters  $\varphi \leftarrow \theta$ ;
18:  end
19: end
20: end

```

References

- Zhang et al., K., 2022. Transformer-based reinforcement learning for pickup and delivery problems with late penalties. *IEEE Trans. on ITS* 23, 24649–24661.
- Alexander, S., et al., 2014. Multi-period cooperative vehicle routing games. *Contributions to Game Theory and Management* 7, 349–359.
- Boeing, G., 2017. Osmnx: New methods for acquiring, constructing, analyzing, and visualizing complex street networks. *Computers, Environment and Urban Systems* 65, 126–139.
- Bogyrbayeva, A., Meraliyev, M., Mustakhov, T., Dauletbayev, B., . Learning to solve vehicle routing problems: a survey (2022). arXiv preprint arXiv:2205.02453 .
- Chalkiadakis, G., Elkind, E., Wooldridge, M., 2022. Computational aspects of cooperative game theory. Springer Nature.
- Chu, H., Zhang, W., Bai, P., Chen, Y., 2021. Data-driven optimization for last-mile delivery. *Complex & Intelligent Systems* , 1–14.
- Colajanni, G., Daniele, P., Nagurney, A., 2023. Centralized supply chain network optimization with uav-based last mile deliveries. *Transportation Research Part C: Emerging Technologies* 155, 104316.

- Drori, I., Kharkar, A., Sickinger, W.R., Kates, B., Ma, Q., Ge, S., Dolev, E., Dietrich, B., Williamson, D.P., Udell, M., 2020. Learning to solve combinatorial optimization problems on real-world graphs in linear time, in: 2020 19th IEEE International Conference on Machine Learning and Applications (ICMLA), IEEE. pp. 19–24.
- Elsayed, M., Mohamed, M., 2020. The impact of airspace regulations on unmanned aerial vehicles in last-mile operation. *Transportation Research Part D: Transport and Environment* 87, 102480.
- Fellek, G., Farid, A., Gebreyesus, G., Fujimura, S., Yoshie, O., 2023. Graph transformer with reinforcement learning for vehicle routing problem. *IEEE Transactions on Electrical and Electronic Engineering* 18, 701–713.
- Fortune, B., 2023. Delivery robots market size, share, and growth. <https://www.marketsandmarkets.com/Market-Reports/delivery-robot-market-263997316.html/>. Accessed: 2024-10-20.
- Fuentes, D., del Blanco, C.R., Jaureguizar, F., Navarro, J.J., García, N., 2023. Solving routing problems for multiple cooperative unmanned aerial vehicles using transformer networks. *Engineering Applications of Artificial Intelligence* 122, 106085.
- Gao, L., Chen, M., Chen, Q., Luo, G., Zhu, N., Liu, Z., 2020. Learn to design the heuristics for vehicle routing problem. arXiv preprint arXiv:2002.08539 .
- Jahanshahi, H., Bozanta, A., Cevik, M., Kavuk, E.M., Tosun, A., Sonuc, S.B., Kosucu, B., Başar, A., 2022. A deep reinforcement learning approach for the meal delivery problem. *Knowledge-Based Systems* 243, 108489.
- James, J., Yu, W., Gu, J., 2019. Online vehicle routing with neural combinatorial optimization and deep reinforcement learning. *IEEE Transactions on Intelligent Transportation Systems* 20, 3806–3817.
- Johnson, G.L., 1985. *Wind energy systems*. Citeseer.
- Kimon, P., George, J., 2015. *Handbook of unmanned aerial vehicles*.
- Kool, W., Van Hoof, H., Welling, M., 2018. Attention, learn to solve routing problems! arXiv preprint arXiv:1803.08475 .
- Lei, K., Guo, P., Wang, Y., Wu, X., Zhao, W., 2022. Solve routing problems with a residual edge-graph attention neural network. *Neurocomputing* 508, 79–98.
- Li, F., Kunze, O., 2023. A comparative review of air drones (uavs) and delivery bots (sugvs) for automated last mile home delivery. *Logistics* 7, 21.
- Li, J., Liu, H., Lai, K.K., Ram, B., 2022. Vehicle and uav collaborative delivery path optimization model. *Mathematics* 10, 3744.
- Li, J., Xin, L., Cao, Z., Lim, A., Song, W., Zhang, J., 2021. Heterogeneous attentions for solving pickup and delivery problem via deep reinforcement learning. *IEEE Transactions on Intelligent Transportation Systems* 23, 2306–2315.
- Liu, R., Shin, H.S., Tsourdos, A., 2023. Edge-enhanced attentions for drone delivery in presence of winds and recharging stations. *Journal of Aerospace Information Systems* 20, 216–228.
- Liu, Y., 2019. An optimization-driven dynamic vehicle routing algorithm for on-demand meal delivery using drones. *Computers & Operations Research* 111, 1–20.
- Ma, Y., Li, J., Cao, Z., Song, W., Guo, H., Gong, Y., Chee, Y.M., 2022. Efficient neural neighborhood search for pickup and delivery problems. arXiv preprint arXiv:2204.11399 .
- Mak, S., Xu, L., Pearce, T., Ostroumov, M., Brintrup, A., 2023. Fair collaborative vehicle routing: A deep multi-agent reinforcement learning approach. *Transportation Research Part C: Emerging Technologies* 157, 104376.
- Mao, X., Wen, H., Zhang, H., Wan, H., Wu, L., Zheng, J., Hu, H., Lin, Y., 2023. Drl4route: A deep reinforcement learning framework for pick-up and delivery route prediction, in: *Proceedings of the 29th ACM SIGKDD Conference on Knowledge Discovery and Data Mining*, pp. 4628–4637.
- Mehra, A., Saha, S., Raychoudhury, V., Mathur, A., 2023. Deliverai: Reinforcement learning based distributed path-sharing network for food deliveries. arXiv preprint arXiv:2311.02017 .
- Nazari, M., Oroojlooy, A., Snyder, L., Takác, M., 2018. Reinforcement learning for solving the vehicle routing problem. *Advances in neural information processing systems* 31.
- Osicka, O., Guajardo, M., van Oost, T., 2020. Cooperative game-theoretic features of cost sharing in location-routing. *International Transactions in Operational Research* 27, 2157–2183.
- Osler, Hoskin, H., 2021. Drone law in canada. URL: https://www.osler.com/osler/media/Osler/infographics/CG5049_Drone-Law-Canada.pdf. accessed: 2023-11-30.
- Ostermeier, M., Heimfarth, A., Hübner, A., 2023. The multi-vehicle truck-and-robot routing problem for last-mile delivery. *European Journal of Operational Research* 310, 680–697.
- Rabecq, B., Chevrier, R., 2022. A deep learning attention model to solve the vehicle routing problem and the pick-up and delivery problem with time windows. arXiv preprint arXiv:2212.10399 .
- Roger, B.M., et al., 1991. *Game theory: analysis of conflict*. The President and Fellows of Harvard College, USA 66.
- Ruland, K., Rodin, E., 1997. The pickup and delivery problem: Faces and branch-and-cut algorithm. *Computers & mathematics with applications* 33, 1–13.
- Samouh, F., Gluza, V., Djavadian, S., Meshkani, S., Farooq, B., 2020. Multimodal autonomous last-mile delivery system design and application, in: 2020 IEEE International Smart Cities Conference (ISC2), IEEE. pp. 1–7.
- Santiyuda, G., Wardoyo, R., Pulungan, R., Vincent, F.Y., 2024. Multi-objective reinforcement learning for bi-objective time-

- dependent pickup and delivery problem with late penalties. *Engineering Applications of Artificial Intelligence* 128, 107381.
- Savelsbergh, M.W., Sol, M., 1995. The general pickup and delivery problem. *Transportation science* 29, 17–29.
- Shapley, L.S., 1967. On balanced sets and cores. *Naval research logistics quarterly* 14, 453–460.
- Shapley, L.S., 1971. Cores of convex games. *International journal of game theory* 1, 11–26.
- Son, J., Kim, M., Choi, S., Park, J., 2023. Solving np-hard min-max routing problems as sequential generation with equity context. arXiv preprint arXiv:2306.02689 .
- Soroka, A., Meshcheryakov, A., Gerasimov, S., 2023. Deep reinforcement learning for the capacitated pickup and delivery problem with time windows. *Pattern Recognition and Image Analysis* 33, 169–178.
- Stolaroff, J.K., Samaras, C., O’Neill, E.R., Lubers, A., Mitchell, A.S., Ceperley, D., 2018. Energy use and life cycle greenhouse gas emissions of drones for commercial package delivery. *Nature communications* 9, 409.
- Sudbury, A.W., Hutchinson, E.B., 2016. A cost analysis of amazon prime air (drone delivery). *Journal for Economic Educators* 16, 1–12.
- Sutton, R.S., McAllester, D., Singh, S., Mansour, Y., 1999. Policy gradient methods for reinforcement learning with function approximation. *Advances in neural information processing systems* 12.
- Veličković, P., Cucurull, G., Casanova, A., Romero, A., Lio, P., Bengio, Y., 2017. Graph attention networks. arXiv preprint arXiv:1710.10903 .
- Williams, R.J., 1992. Simple statistical gradient-following algorithms for connectionist reinforcement learning. *Machine learning* 8, 229–256.
- Xiao, X., Whittaker, W., 2014. Energy considerations for wheeled mobile robots operating on a single battery discharge. *Robot. Inst., Carnegie Mellon Univ., Pittsburgh, PA, USA, Tech. Rep., CMU-RI-TR-14-16 .*
- Zhang, K., Li, M., Wang, J., Li, Y., Lin, X., 2023a. A two-stage learning-based method for large-scale on-demand pickup and delivery services with soft time windows. *Transportation Research Part C: Emerging Technologies* 151, 104122.
- Zhang, K., Lin, X., Li, M., 2023b. Graph attention reinforcement learning with flexible matching policies for multi-depot vehicle routing problems. *Physica A: Statistical Mechanics and its Applications* 611, 128451.
- Zibaei, S., Hafezalkotob, A., Ghashami, S.S., 2016. Cooperative vehicle routing problem: an opportunity for cost saving. *Journal of Industrial Engineering International* 12, 271–286.
- Zong, Z., Zheng, M., Li, Y., Jin, D., 2022. Mapdp: Cooperative multi-agent reinforcement learning to solve pickup and delivery problems, in: *Proceedings of the AAAI Conference on Artificial Intelligence*, pp. 9980–9988.